

CURE KINETICS MODELLING AND CURE SHRINKAGE BEHAVIOUR OF
AS4/8552

by

Mehmet Tuğutlu

B.S., Mechanical Engineering, Boğaziçi University, 2005

Submitted to the Institute for Graduate Studies in
Science and Engineering in partial fulfillment of
the requirements for the degree of
Master of Science

Graduate Program in Mechanical Engineering
Boğaziçi University

2008

ACKNOWLEDGEMENTS

I would like to acknowledge my advisor Assist. Prof. Nuri Ersoy for offering me his full support.

I would also like to thank Kenan Çınar for his help in all things to do with sample preparation.

Finally, I would like to dedicate my thesis to Kerem Aydınlar, who was my brave, faithful, unique, and complete friend and died recently. He lived in such a good way. I will never forget him. All my compliments to him.

ABSTRACT

CURE KINETICS MODELLING AND CURE SHRINKAGE BEHAVIOUR OF AS4/8552

In this work, the reaction kinetics and through-the-thickness cure shrinkage upon curing of an AS4/8552 epoxy resin system have been studied. The study included two major works. Firstly, dynamic and isothermal experiments were performed to develop a new cure kinetics model using Differential Scanning Calorimetry (DSC). In the dynamic part of the experiments, 1, 2, 3, 4, and 5K/min rates were used. In the isothermal part, 120, 140, 160, and 180°C temperatures were applied for certain durations. The most appropriate kinetic model that produces a nearly perfect fit of the scans of all data sets corresponds to a process with a single-step parallel reaction with diffusion control. The whole curing process was treated to be composed of two cure reactions. The relationship between cure rate and degree of cure was simulated by the autocatalytic twelve-parameters model. The model is a modified version of the Sourour-Kamal equation and also involves the Rabinowitch, Arrhenius, and WLF(Williams Landel Ferry) equations. Multivariant kinetic analysis were used to evaluate the parameters. The predictions of the new model were compared with the results of isothermal experiments by focusing on the degree of cure concept. Also, the glass transition temperatures, the residual heats, and the degree of cure values for each isothermal study were noted separately. The degree of cure values of isothermal experiments can be correctly predicted using the model parameters.

Secondly, the coefficient of thermal expansion, the glass transition temperatures, and the through-the-thickness cure shrinkage strain values of the unidirectional and cross-ply samples, which were precured at 120, 140, 160, and 180°C temperatures isothermally for the durations same as the isothermal DSC experiments in the autoclave, were calculated according to the data obtained by heating from room tem-

perature up to 250°C and cooling back to the room temperature using a Dynamic Mechanical Analyzer (DMA). The T_g (Glass Transition Temperature) values obtained by DSC and DMA samples were compared. The strain values of XP(crossply) samples were always higher than the UD(unidirectional) samples. The T_g values were proportional to the isothermal precure temperature and did not change in accordance with the type of sample (UD or XP). After the whole cure completed, the T_g values were nearly same for all samples. The Coefficient of Thermal Expansion (CTE) values above T_g are much larger than those below T_g . Without some exceptions, the CTE values of XP samples are nearly twice of UD samples. Also, after the curing is completed, the CTE values decreases. The results showed that as the isothermal precure temperature increased the cure shrinkage strain values decreased. Two composite samples (one UD, one XP), which were heated to 120°C and held at 120°C for one hour, were used to investigate the through-the-thickness cure shrinkage strain values of the Manufacturer's Recommended Cure Cycle (MRCC). Also, two completely cured composite samples (one UD, one XP) were tested to find the CTEs and T_g s of fully cured samples.

ÖZET

AS4/8552'NİN KİNETİK KÜRLENME MODELLEMESİ VE KÜRLENME BÜZÜŞMESİ

Bu çalışmada, AS4/8552 epoksi reçine sisteminin pişirme esnasındaki reaksiyon kinetiği ve kalınlığı doğrultusunda kürlenme büzüşmesi incelendi. Çalışma, iki temel iş içermektedir.

İlk olarak, Diferansiyel Taramalı Kalorimetri(DSC) kullanarak yeni bir kürlenme modeli oluşturmak için dinamik ve izotermal deneyler yapıldı. Deneylerin dinamik kısmında, 1, 2, 3, 4, ve 5K/dak ısıtma hızları kullanıldı. İzotermal kısımda, 120, 140, 160, ve 180°C sıcaklıkları belirli süreler için uygulandı. Bütün veri gruplarının ölçümleriyle neredeyse tam bir örtüşme oluşturan en uygun kinetik model, difüzyon kontrollü tek aşamalı paralel reaksiyonlu bir sürece uymaktadır. Kürlenme sürecinin bütünü, iki reaksiyonun bileşimi şeklinde değerlendirildi. Kürlenme hızı ve kürlenme derecesi arasındaki ilişki, otokatalitik olan oniki parametrelilik bir modelle tanımlandı. Model, Sourour-Kamal denkleminin değiştirilmiş bir versiyonudur ve ayrıca Rabinowitch, Arrhenius, ve WLF (Williams Landel Ferry) denklemlerini içerir. Parametreleri bulmak için çok değişkenli kinetik analiz kullanıldı. Kürlenme derecesi kavramına odaklanılarak, yeni modelin tahminleri izotermal deneylerin sonuçlarıyla karşılaştırılmıştır. Ayrıca, her izotermal çalışmanın, camsı geçiş sıcaklığı, artık ısı ve kürlenme derecesi değerleri ayrı ayrı kaydedildi. İzotermal deneylerin kürlenme derecesi değerleri model parametrelerini kullanarak doğru bir şekilde tahmin edilebilmektedir.

İkinci olarak, otoklavda izotermal DSC deneyleriyle aynı süreler boyunca 120, 140, 160 ve 180°C sıcaklıklarda izotermal olarak önceden pişirilmiş tek yönlü ve çapraz dizilmiş numunelerin ısıl genleşme katsayısı, camsı geçiş sıcaklığı ve kalınlığı boyunca kürlenme büzüşmesi değerleri, Dinamik Mekanik Analiz Cihazı(DMA) kullanılıp oda

sıcaklığından 250°C'e kadar ısıtılarak, ardından tekrar oda sıcaklığına soğutularak elde edilmiş verilere göre hesaplanmıştır. DSC ve DMA numunelerinden elde edilen T_g değerleri karşılaştırıldı. XP numunelerin ısı genleşme katsayısı değerleri UD numunelerinkilerden her zaman yüksek çıktı. T_g değerleri izotermal ön kurlenme sıcaklığıyla orantılıydı ve numunelerin tipine (UD yada XP) göre değişmedi. Bütün kurlenme tamamlandıktan sonra T_g değerleri tüm numuneler için neredeyse aynıydı. T_g 'den yukarıdaki sıcaklıklarda Isıl Genleşme Katsayısı(CTE) değerleri, T_g den aşağıdakilerden daha fazlaydı. Bazı istisnalar haricinde, XP numunelerinin CTE değerleri UD numunelerinkilerin hemen hemen iki katıydı. Ayrıca, kurlenme tamamlandıktan sonra CTE değerleri azaldı. Sonuçlar, izotermal önceden kurlenme sıcaklıklarının artmasıyla kurlenme büzüşmesi değerlerinin azaldığını açığa çıkardı. 120°C sıcaklığa ısıtılarak bir saat 120°C 'de tutulmuş iki kompozit numune (bir UD, bir XP), üreticilerce tavsiye edilen kurlenme çevrimlerinin kalınlığı doğrultusunda yol açtığı kurlenme büzüşmesi değerlerini incelemede kullanıldı.

TABLE OF CONTENTS

ACKNOWLEDGEMENTS	iii
ABSTRACT	iv
ÖZET	vi
LIST OF FIGURES	x
LIST OF TABLES	xiv
LIST OF SYMBOLS/ABBREVIATIONS	xvi
1. INTRODUCTION	1
1.1. LITERATURE SURVEY	5
1.1.1. Cure Kinetics	5
1.1.2. Cure Shrinkage	12
1.2. PROBLEM STATEMENT	16
2. EXPERIMENTAL	19
2.1. DSC EXPERIMENTS	19
2.1.1. Experimental Material	19
2.1.2. Testing Equipment	19
2.1.2.1. DSC	19
2.1.3. Procedure	20
2.2. DMA EXPERIMENTS	21
2.2.1. Experimental Material	21
2.2.1.1. Sample preparations	21
2.2.2. Testing Equipment	23
2.2.2.1. DMA	23
2.2.3. Tests	25
3. MODELING	26
3.1. Degree of Cure	26
3.2. Cure Rate	27
3.3. Proposed Model	28
4. RESULTS AND DISCUSSION	32
4.1. DSC STUDY	32

4.1.1. DSC Dynamic Cure Analysis	32
4.1.2. Cure Kinetic Modelling	35
4.1.3. DSC Isothermal Cure Analysis	37
4.1.4. Comparison of Model Predictions and Isothermal Measurements	41
4.2. DMA STUDY	44
4.2.1. Analysis of isothermal results	44
4.2.2. Thermal expansion and cure shrinkage	49
4.2.3. Analysis of MRCC	53
4.2.4. Comparison of Results	56
5. CONCLUSIONS	59
APPENDIX A: MORE DMA STUDY CURVES	62
REFERENCES	64

LIST OF FIGURES

Figure 1.1.	Curing of a thermosetting resin: a) monomer stage, b) linear growth and branching, c) formation of gelled but incompletely cross-linked network, d) fully cured thermoset . [1]	2
Figure 1.2.	Heat flow of reaction in curing process	4
Figure 1.3.	Through-the-thickness strain induced by consolidation and cure shrinkages [2]	4
Figure 1.4.	Manufacturer's Recommended Cure Cycle	18
Figure 2.1.	Specimen on compression clamps used in the DMA	24
Figure 3.1.	Single-step parallel reaction model	29
Figure 3.2.	The relationship between T_g and α for AS4/8552 composite	31
Figure 4.1.	Nonreversible heat flow vs. temperature graphs of prepregs cured by 1 ,2 , 3, 4, and 5 K/min dynamic rates	33
Figure 4.2.	Nonreversible heat flow vs. time graphs of prepregs cured by 1, 2, 3, 4, and 5 K/min dynamic rates	34
Figure 4.3.	Integration method to calculate the curing heat of reaction for 1 K/min dynamic experiment as an example	34
Figure 4.4.	Nonreversible heat flow vs. time graph of prepregs cured by 1, 2, 3, 4, and 5 K/min dynamic rates respectively, with model fit shown as continues curves	36

Figure 4.5.	Heat flow vs. time graphs of the isothermal experiments; the heats of reaction are the peaks at the left; the residual heats are the peaks at the right	37
Figure 4.6.	Nonreversible and reversible heat flow vs. time graphs during reheating stage of prepregs cured isothermally at 120; T_g value found by reversible heat flow curve; residual heat found by nonreversible heat flow curve	38
Figure 4.7.	Nonreversible and reversible heat flow vs. time graphs during reheating stage of prepregs cured isothermally at 140°C; T_g value found by reversible heat flow curve; residual heat found by nonreversible heat flow curve	39
Figure 4.8.	Nonreversible and reversible heat flow vs. time graphs during reheating stage of prepregs cured isothermally at 160°C; T_g value found by reversible heat flow curve; residual heat found by nonreversible heat flow curve	39
Figure 4.9.	Nonreversible and reversible heat flow vs. time graphs during reheating stage of prepregs cured isothermally at 180°C; T_g value found by reversible heat flow curve; residual heat found by nonreversible heat flow curve	40
Figure 4.10.	Isothermal predictions of the model based on dynamic experiments	42
Figure 4.11.	Heat flow vs. time graphs of the isothermal experiments	42
Figure 4.12.	Isothermal predictions of the model according to the cure kinetics model; A=uncured part, B=cured part	43
Figure 4.13.	Isothermal predictions of the model according to cure kinetics model	44

Figure 4.14. Displacement vs. temperature graphs of heating and cooling cycle of XP and UD samples precured isothermally for 180°C, together with the thermal response of the empty clamp	45
Figure 4.15. Strain vs. temperature graphs of cross-ply and unidirectional samples precured isothermally for 120°C; including both heating and cooling stages	46
Figure 4.16. Strain vs. temperature graphs of cross-ply and unidirectional samples precured isothermally for 140°C; including both heating and cooling stages	46
Figure 4.17. Strain vs. temperature graphs of cross-ply and unidirectional samples precured isothermally for 160°C; including both heating and cooling stages	47
Figure 4.18. Strain vs. temperature graphs of cross-ply and unidirectional samples precured isothermally for 180°C; including both heating and cooling stages	47
Figure 4.19. T_g calculations from the DMA experiments for 160XP sample as an example	48
Figure 4.20. CTE calculations from the DMA experiments for 160XP sample as an example	49
Figure 4.21. Strain vs. time graph of composites precured isothermally for 120°C	50
Figure 4.22. Strain vs. time graph of composites precured isothermally for 140°C	51
Figure 4.23. Strain vs. time graph of composites precured isothermally for 160°C	51

Figure 4.24.	Strain vs. time graph of composites precured isothermally for 180°C	52
Figure 4.25.	The method of calculating the cure shrinkage; displacement vs temperature graph of the sample precured at 140°C, as an example . .	53
Figure 4.26.	The method of calculating the cure shrinkage; displacement vs time graph of UD samples subjected to MRCC	55
Figure 4.27.	The method of calculating the cure shrinkage; displacement vs time graph of XP samples subjected to MRCC	55
Figure 4.28.	Strain vs. temperature graph of UD and XP samples subjected to MRCC	57
Figure 4.29.	Strain vs. temperature graph of UD and XP samples of completely cured samples	57
Figure A.1.	Strain vs. temperature graphs of full cycles of unidirectional DMA samples precured isothermally for 120, 140, 160, and 180°C; including both heating and cooling stages	62
Figure A.2.	Strain vs. temperature graphs of full cycles of unidirectional DMA samples precured isothermally for 120, 140, 160, and 180°C; including both heating and cooling stages	63

LIST OF TABLES

Table 2.1.	Properties of AS4/8552	19
Table 2.2.	Prepreg sample mass for dynamic experiments	21
Table 2.3.	Prepreg sample mass for isothermal experiments	21
Table 2.4.	Time intervals for isothermal experiments	23
Table 3.1.	Parameters of the model	30
Table 4.1.	Total heat of reaction values for dynamic experiments	35
Table 4.2.	Parameter values of the model; found by the nonlinear regression analysis of the software	36
Table 4.3.	Glass transition temperatures from reversible and nonreversible heat flow measurements of prepreg for isothermal experiments	40
Table 4.4.	Isothermal heat of reaction, residual heat of reaction, measured and predicted degrees of cure, and glass transition temperatures of samples precured isothermally	41
Table 4.5.	T_g values from DMA experiments	48
Table 4.6.	CTE values from DMA experiments	50
Table 4.7.	Cure shrinkage values calculated from the thermal response of the samples during heating	54

Table 4.8.	Cure shrinkage strain values of MRCC	54
Table 4.9.	Comparison of T_g values from the measurements of DMA experiments and the CTE values of the completely cured samples	56
Table 4.10.	Comparison of T_g values from DSC and DMA experiments	58

LIST OF SYMBOLS/ABBREVIATIONS

α	Degree of cure
T	Temperature
t	Time
K	Kelvin
T_g	Glass transition temperature
C	Celcius
E_a	Activation energy
R	Universal gas constant
k_0	Pre-exponential factor
A_i	Pre-exponential factor
n_i	Reaction order
ΔE	Activation energy
n	Reaction order
K_0	Pre-exponential factor
α_{C0}	critical degree of cure at T=0K
α_{CT}	increase in critical resin degree of cure with temperare T
ε_{cure}	Cure shrinkage strain
C	Diffusion factor
A	Pre-exponential factor
α_C	critical degree of cure at T=0K
K_{cat}	Autocatalytic reaction constant
H_R	Residual heat of reaction
H_U	Ultimate heat of reaction
H_T	Isothermal heat of reaction
H_t	Partial heat of reaction at time t
CTE	Coefficient of thermal expansion
DSC	Differential scanning calorimeter
DMA	Dynamic mechanical analyser

MDSC	Modulated differential scanning calorimeter
MRCC	Manufacturer's recommended cure cycle
PID	Proportional integral derivative
TMA	Thermomechanical analyser
XP	Cross-ply
UD	Unidirectional
WLF	Williams Landel Ferry

1. INTRODUCTION

Composite materials are being used in the industry at an increasing rate because of their superior properties. The composites, which are composed of a continuous reinforcing fiber and a polymer matrix resin, have desirable chemical and physical specifications. They have high strength and can compensate specific strength requirements in aerospace applications. Recording rigidity, they have high stiffness and satisfy the low deformation requirement under high load. Compared to steel and aluminum, they are light materials which have the highest ratio of strength to weight. Also they have excellent resistance against corrosion and wearing. On account of these unique chemical and physical properties, the composites find applications in many areas such as spacecraft, aircraft, marine, etc. For some applications, composite materials are considered to be more suitable than conventional materials as they have favorable mechanical and thermal properties.

The reinforcing fiber and the matrix resin are bonded together with interfaces which greatly determine the mechanical and physical properties of composite materials. The matrix resin is binding agent of the composites that covers the fibers. The matrix supports and protects the fibers which carry the majority of the loading.

The matrix material can be either thermosets or thermoplastics. In thermosets, the liquid resin changes its phase to hard and brittle solid with the application of heat. Phase change occurs by chemical cross-linking reactions which induce 3D network of polymer chains. This can be seen in Figure 1.1 [1]. In thermoplastics, the application of heat leads to melting of material. They have linear molecular chains and can be reformed. Thermoset materials once cured cannot be remelted or reformed. During cure cycle, they form 3D molecular network, called cross-linking. Due to these cross-links, the molecules are not flexible and cannot be remelted and reshaped. The higher the number of cross-linkings, the more rigid and thermally stable the material will be. Thermosets offer greater thermal and dimensional stability, better rigidity, and higher electrical, and solvent resistance. The most common resin material used

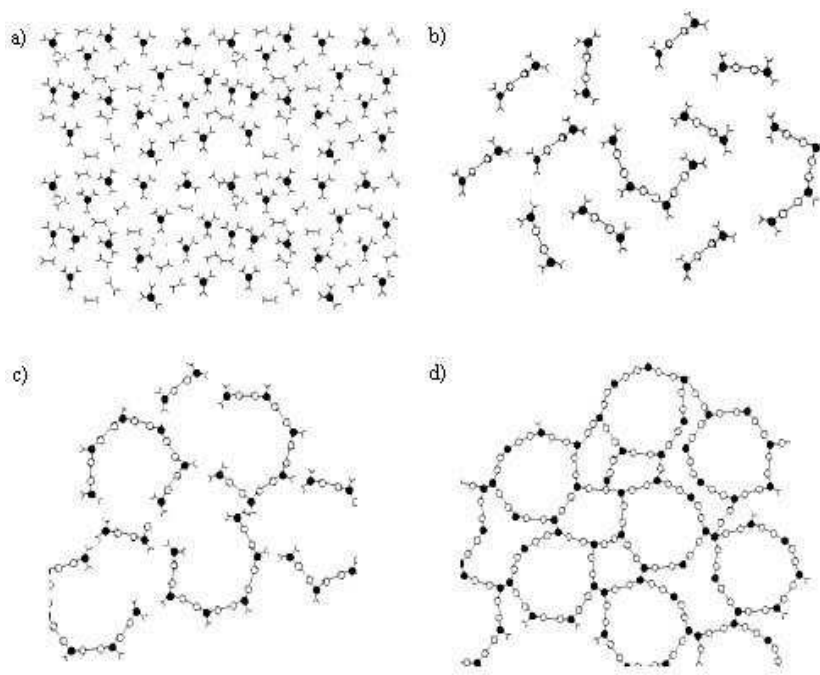


Figure 1.1. Curing of a thermosetting resin: a) monomer stage, b) linear growth and branching, c) formation of gelled but incompletely cross-linked network, d) fully cured thermoset . [1]

in thermoset composites is epoxy. Epoxies are the most widely used resin materials and are used in many applications, from aerospace to sporting goods. A prepreg is a resin-impregnated fiber. Fibers laid at 0° orientation and preimpregnated with resin are called unidirectional tape. A unidirectional tape provides the ability to tailor the composite properties in the desired direction. These prepregs are generally stored in a low-temperature environment and have a limited shelf life. Thermoset prepregs require a longer process cycle time with respect to thermoplastics, typically in the range of 1 to 8 hours due to their slower kinetic reactions. Epoxy resins and epoxy prepreg are important thermosetting polymers. Curing cycles determine the degree of cure of epoxy prepreg and have an important effect on the mechanical properties of the final products. Optimal curing methods are important to achieve the desired properties of the cured materials. Already small variations in the cure schedule may damage the material leading to low performance, delamination, warpage, or matrix cracking. During the curing process the epoxy resin is becoming chemically crosslinked. Therefore, it undergoes changes from a liquid to a rubber-like material before reaching the final stage of glassy solid. The network formation is inevitably linked to volume shrinkage.

Because of these, it is necessary to understand the cure kinetics and characteristics of epoxy prepreg in detail.

Carbon fiber-reinforced epoxy matrix composites are used extensively in aerospace and other structural applications because of their high strength, high stiffness, and low density. In this study, the resin of choice is Hexcel 8552 which is commonly used in aerospace composite structures.

Various methods were used to analyze the cure kinetics of epoxy prepreg in this study. First one was DSC (Differential Scanning Calorimeter) analysis which is based on the heat flow change of the epoxy prepreg sample during the cure process. In this study, dynamic and isothermal analysis were performed to investigate cure kinetics. In the dynamic experiments, temperature was increased gradually to a specific degree. In the isothermal experiments, temperature was fixed to a certain degree and held by a specific time interval.

The chemical reactions involved in the cure of a resin such as 8552 result in the generation of heat, as low molecular weight monomers are converted into highly cross-linked polymeric structure. The degree of cure is proportional to the heat of reaction as shown in Figure 1.2. So, it is calculated by either residual heat or by the reaction heat at a particular time. Second step was modeling the cure behaviour with appropriate approaches and parameters.

DMA (Dynamic Mechanical Analyser) is used to understand the through-the-thickness thermal behaviour of the composite samples. The DMA study is focused on Coefficient of Thermal Expansion (CTE), glass transition temperature (T_g), and cure shrinkage values. First composite samples were prepared from epoxy prepreps. Then predetermined cycles were applied to the samples. Garstka et. al [2] divided the development of the through-thickness strain in AS4/8552 composite during the Manufacturer's Recommended Cure Cycle (MRCC) into five steps as shown in Figure

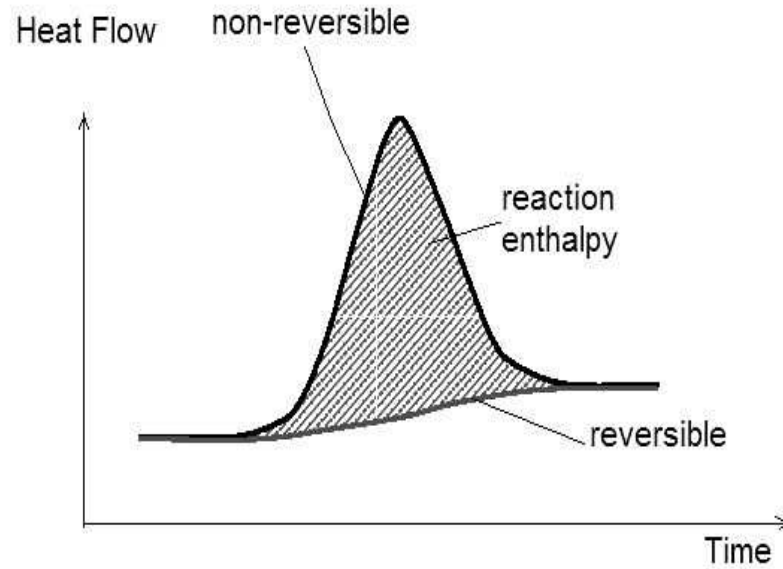


Figure 1.2. Heat flow of reaction in curing process

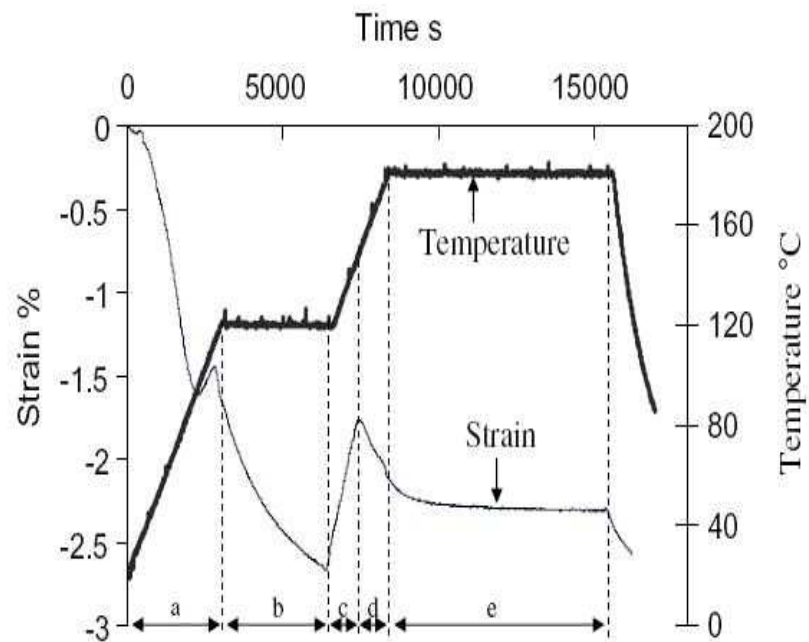


Figure 1.3. Through-the-thickness strain induced by consolidation and cure shrinkages [2]

1.3.

In the first stage designated as 'a' the temperature is increasing at 2°C/min, and the through-thickness strain is driven by two competing mechanisms: liquid thermal expansion of the resin and consolidation. Cure has not yet advanced sufficiently to cause chemical shrinkage. In stage 'b', since the temperature is constant at 120°C, the strain decreases mostly due to consolidation processes and a small amount of chemical shrinkage. In stage 'c' the curing strain is affected by three competing mechanisms: chemical shrinkage of the resin, thermal expansion, and consolidation. At the beginning of stage 'd' the resin gels, as confirmed by the knowledge of the AS4-8552 cure kinetics. In stage 'd' the through-thickness strain is affected by resin shrinkage and thermal expansion. The observed sudden change in slope at the beginning of stage 'd' is a result of the cure shrinkage and reduction of the material thermal expansion coefficient which occurs when the material transforms from a liquid to a rubbery state. In stage 'e' the temperature is constant at 180°C and the resin has passed the gel point. It can be assumed that the consolidation mechanisms can no longer take place, and through-thickness strain is driven only by the chemical shrinkage of the resin [2].

1.1. LITERATURE SURVEY

1.1.1. Cure Kinetics

Opalicki et al. [3] perform dynamic and isothermal experiments using 8552 resin with 33 % carbon fiber. Mettler TA300 DSC device was used to complete dynamic part of the experiment. Measurement types were peak areas and straight line baselines. Proposed model was:

$$\frac{d\alpha}{dt} = k(\alpha + B)(1 - \alpha)(r - \alpha) \quad (1.1)$$

$$k = k_0 \exp\left(\frac{-E_a}{RT}\right) \quad (1.2)$$

where α was degree of cure, E_a was activation energy, R was universal gas constant, T was temperature, $r=1$, k_0 was pre-exponential factor, t is time, k and B values were different for various temperatures.

Buczek et al. [4] measured curing of S2/8552 glass-epoxy composite and proposed a two-reaction model:

$$\frac{d\alpha}{dt} = \sum \frac{d\alpha_i}{dt} = K_i(1 - \alpha_i)^{n_i} \quad (1.3)$$

$$K_i = A_i e^{\frac{-\Delta E}{RT}} \quad (1.4)$$

where A_i was pre-exponential factor, n_i was reaction order, $-\Delta E$ was activation energy.

Player et al. [5] proposed one reaction model for 8552 resin. The model was:

$$\frac{d\alpha}{dt} = K(1 - \alpha)^n \quad (1.5)$$

$$K = K_0 e^{\frac{-E}{RT}} \quad (1.6)$$

where n was reaction order, K_0 was pre-exponential factor.

Hubert et al. [6] measured isothermal and dynamic residuals of 8552 resin using PE DSC 7 device. The experiments were performed at 130, 150, and 170°C. One reaction model with a diffusion factor was proposed. Also the diffusion factor was associated with temperature. The model was:

$$\frac{d\alpha}{dt} = \frac{K(1 - \alpha)^n}{1 + e^{C[\alpha - (\alpha_{C0} + \alpha_{CT}T)]}} \quad (1.7)$$

$$K = Ae^{-\frac{\Delta E}{RT}} \quad (1.8)$$

C was diffusion factor, α_{C0} was critical degree of cure at T=0K, α_{CT} was constant accounting for increase in critical resin degree of cure with T, A was pre-exponential factor.

Antonucci et al. [7] tested 8552 and developed a model with two reactions:

$$\frac{d\alpha}{dt} = (e^{4.438 - \frac{5990}{T}} + e^{11.69 - \frac{7783}{T}} \alpha)(1 - \alpha)^{2.24} + e^{56.16 - \frac{31580}{T}} (1 - \alpha)^{1.219} \quad (1.9)$$

Sun et al. developed two separate models according to isothermal and dynamic behaviour of 8552 with 33% carbon fiber. The isothermal tests were performed in the range of 110 C and 220°C using Seiko DSC. The dynamic ones were completed with 2, 5, 10, 15, and 20°C/min intervals using Seiko DSC. Isothermal model was developed with one reaction including diffusion factor. Dynamic model consists of two reactions which were autocatalytic and n^{th} order reactions.

The isothermal model was [8]:

$$\frac{d\alpha}{dt} = \frac{(k_1 + k_2\alpha^m)(1 - \alpha)^n}{1 + e^{C(\alpha - \alpha_C)}} \quad (1.10)$$

$$k_i = A_i e^{-\frac{E}{RT}} \quad (1.11)$$

C is diffusion factor, α_C is critical degree of cure at T=0K. The dynamic model was[9]:

$$\frac{d\alpha}{dt} = \left(\frac{dT}{dt}\right)^{-1} K_i (\alpha_1 + \alpha_2)^{m_i} (1 - \alpha_1 - \alpha_2)^{n_i} \quad (1.12)$$

$$K_i = A_i e^{-\frac{E}{RT}} \quad (1.13)$$

A , E , m , n values were different for various ($\frac{dT}{dt}$)

Ersoy et al. [10] measured 8552 resin using dynamic residuals. TA Instruments 2920 MDSC (Modulated Dynamical Scanning Calorimeter) was used to perform the tests. One reaction model with diffusion factor was proposed and the diffusion factor was associated with temperature as the Hubert model. The model was:

$$\frac{d\alpha}{dt} = \frac{K(1 - \alpha)^n}{1 + e^{C[\alpha - (\alpha_{C0} + \alpha_{CT}T)]}} \quad (1.14)$$

$$K = Ae^{\frac{-\Delta E}{RT}} \quad (1.15)$$

C is diffusion factor, α_{C0} is critical degree of cure at $T=0K$, α_{CT} is constant accounting for increase in critical resin degree of cure with T .

Flammersheim [12] measured a 1:1 mixture of bisphenol-A-diglycidyl ether and N, N'-dibenzyl-4,4'-diaminodiphenyl-methane using DSC. The proposed model included two competitive reactions as in Eq.1.16:



The model was:

$$-\frac{de}{dt} = A_1 e^{\frac{-E_{A,1}}{RT}} (e)^2 + A_2 e^{\frac{-E_{A,2}}{RT}} (e)^n p^m \quad (1.17)$$

where e and p are the concentrations of reactant and product, A and E_A the

Arrhenius parameter and n and m are the formal reaction orders.

Flammersheim et al. [12] measured a 1:1 mixture of bisphenol-A-diglycidyl ether and N, N'-dibenzyl-4,4'-diaminodiphenyl-methane using DSC, again. Three models were studied. The most simple formal-kinetic model that produced a nearly perfect fit corresponded to a process with two competitive reactions. The rate law was then:



$$-\frac{d\alpha}{dt} = A_1 e^{\frac{-E_{A,1}}{RT}} (1 - \alpha)^2 + A_2 e^{\frac{-E_{A,2}}{RT}} (1 - \alpha)^n \alpha^m \quad (1.19)$$

where n and m are the formal reaction orders. The second model consisted of two independent, autocatalytic concurrent reactions and the rate law was:



$$-\frac{d\alpha_{1,2}}{dt} = A_{1,2} e^{\frac{-E_{A,1,2}}{RT}} (1 - \alpha_{1,2})^n (1 + K_{cat,1,2} \alpha_{1,2}) \quad (1.21)$$

where K_{cat} considers the autocatalysis by the reaction products. The third kinetic model that produced a practically perfect fit for all heating rates corresponded to a

process with two consecutive partial steps.



$$-\frac{d\alpha_B}{dt} = A_1 e^{\frac{-E_{A,1}}{RT}} \alpha_A^{n_1} - A_2 e^{\frac{-E_{A,2}}{RT}} \alpha_B^{n_2} (1 + K_{cat,2} \alpha_C) \quad (1.23)$$

Flammersheim et al. [11] measured a commercial epoxy (RUETAPOX VE 3579) using MDSC. The Rabinowitch [13] and modified WLF type [14] equations were utilized. The most simple model that produced a practically perfect fit of the experimental data of the study corresponded to a process with two consecutive partial steps as in Eq.1.22 and the model was:

$$-\frac{d\alpha_B}{dt} = A_2 e^{\frac{-E_{A,2}}{RT}} \alpha_B^{n_2} (1 + K_{cat} \alpha_C) \quad (1.24)$$

Only the second step of the reaction was influenced by the diffusion. As a trial, the diffusion control was not used, no acceptable fit was reached.

There is a significant variation among the mentioned model predictions. Sun et al. [9] have suggested the cure kinetics model should really be the addition of two models for two reactions that take place during the cure of 8552 resin. Buczek et al. [4] have also suggested the addition of two or more reactions in their models. The model proposed by Antonucci et al.[7] also appears to express two reactions, although confirmation of such finding is not available at this time. Sun et al.[9] used a test

method involving temperature ramps rather than isothermal holds. The experimental method behind the dynamic model consists of a series of temperature ramps (no isothermal holds) at various heating rates, and recording of the temperature at the heat flow peaks for a consistent degree of cure. This technique allows for separation of multiple reactions such that their unique activation energies can be found.

The Sun dynamic model used a combination of area under the peak calculations, and peak temperatures to formulate the cure model. Consequently, the model was dependent on heating rate.

The variety of models also stem from different model fitting methods. Some models have a single set of parameter values that are a result of averaging over the entire experimental data set, whereas others have a set of parameter values for each isothermal temperature or heating rate. Different methods for finding the parameter values exist: the Superposition or Arrhenius plot methods are used for isothermal tests; the Kissinger and Ozawa, and Borchardt and Daniels approaches are used for dynamic tests.

The difference between the models also stem from the factors added to express diffusion control. Ersoy et al. [10] and Hubert et al. [6] used the same model. Sun et al. [8] used a similar denominator but do not include a constant accounting for increase in critical resin degree of cure with temperature. Antonucci et al. [7] used a rate limiting mobility factor. Only Ersoy et al., Hubert et al., and Sun et al. models have been normalized to a degree of cure at which the cure rate decreases dramatically before reaching a value of unity due to their diffusion parameters.

Sun et al. [8] and Antonucci et al. [7] choose a model that combines n^{th} order and autocatalytic reactions, and hence initial rate of cure is greater than zero at time zero. Opalicki et al. used a mechanistic model that also expresses n^{th} order behaviour at the beginning of the reaction. The other models have used autocatalytic reactions starting at zero rate of cure at time zero.

1.1.2. Cure Shrinkage

Yates et al. [15] worked on cure shrinkage of Derakane 411-48/MEKP, Epikote 828/MNA/BDMA and XB2878A/XB2878B and DLS351/BF3400 while reporting the curing cycles of the resins. Conclusions were drawn concerning: such as the overall percentage volume contraction during cure; the shape and time-scale of the curing characteristics in relation to the state of completion of the curing process; the approximate location of the temperature below which no further shrinking due to polymerization or cross-linking is likely to occur, etc. A manometer dilatometer was used to get results.

Daniel et al. [16] dealt with the warpage of prepreg cured on an identical layer of the same material that had already been cured and post-cured. The shadow Moire method was applied to calculate the chemical shrinkage.

Igarashi et al. [17] studied the contractive stresses of amine curing epoxy resin during isothermal curing. Photoelastic and bimetallic methods were used for measuring the increase in elastic modulus during the curing process of the resin. The contractive stress in composite systems was observed only after gelation of the resin. The volume contraction after gelation was effective in generating contractive stress; the contraction in the fluid state was not effective. The effective contraction was estimated to be one third of the total contraction in this experiment.

Russell [18] dealt with shrinkage of AS4 carbon fibre/Hercules 3501-6 epoxy, and IM7 carbon fibre/Hercules 8551-7A toughened epoxy, and IM7 carbon fibre/BASF 5250-4 bismaleimide. Dynamic Mechanical Analysis (DMA) and dielectric cure monitoring techniques were used to get the results of volume changes of the materials during cure. Then results from different techniques were compared.

Jonston [19] studied AS4/8552 composite and performed two sets of experiments on it. Firstly, TMA (Thermomechanical Analyser) was used to calculate ply cure shrinkage strains from continuous measurements of the change in dimension of the test specimen during cure. Secondly, effective cure shrinkage strains were examined at the

completion of a test. Measured effective cure shrinkage strains were more than an order of magnitude lower than the total cure shrinkage strains obtained by TMA.

Stone et. al. [20] measured in situ the chemical shrinkage of a low temperature cure resin system after gelation. Density column technique was used. A bimaterial specimen experiment was developed to isolate the chemical and thermal contribution to curvature.

Prasatya et al. [21] used a pressurisable bellows dilatometer to measure chemical shrinkage of Hexcel 8551-7 thermoset epoxy. The experiments were performed at a constant temperature of 122 and 5MPa pressure.

Horng-Jer Tai. [22] studied the reaction kinetics with a diffusion control mechanism, as well as the volumetric change upon curing, of a cresol novolac epoxy/o-cresol-formaldehyde novolac hardener system. Simple equations to model the change in linear coefficients of thermal expansion with reacting thermosetting system conversion were also derived. The reaction is modeled as a reaction of shifting order: it first reacts autocatalytically and later switches into diffusion control. The reaction in the diffusion-controlled region were modeled by an n-th order kinetic equation with its rate constant described by a WLF-type equation. Both experimental linear coefficients of thermal expansion above and below the glass transition temperature decreased linearly with the degree of conversion, which agreed with the derived equations. The importance of chemical shrinkage upon curing was also discussed.

Bilyeu et al. [23] studied the volume changes of epoxy prepregs. A quartz dilatometry cell inside a TMA system was used to perform the experiments. Compression was applied at a temperature higher than the T_g to isolate void elimination volume change whereas the change due to reaction shrinkage was observed at a longer time at the cure temperature. Uniaxial and biaxial composite prepregs were studied. Each sample exhibited approximately 0.5% volume change due to cross-linking. Void elimination varied with temperature, pressure and fiber orientation. Higher pressure resulted in higher void elimination. Lower cure temperature procedure higher void elimination.

Zarrelli et al. [24] studied the coefficients of chemical shrinkage. TGDDM resin was used as an experimental material. Testing equipment was liquid dilatometry at different curing temperatures. Tests at different temperatures showed the same response of the specific volume change. A linear relationship between chemical shrinkage and degree of cure was fitted to the experimental data. There were no further specific volume variations when the resin reached the vitrification point at different temperatures. In the three cases in which measurements were possible over the entire curing cycle it was established that major shrinkage occurs during the early stages of solidification, although the shrinkage characteristics vary in detail from one resin to another.

Li et al. [25] applied a different system to measure in situ chemical shrinkage of epoxy resins pass through-the-liquid, rubbery and glassy states. A small sample of MY750/HY917/DY073 epoxy resin system, sealed in a thin-walled silicon rubber bag, was suspended in a pot of silicone fluid and weighed independently of the silicon bath. The buoyancy of the sample was monitored as its density increased with respect to the constant density fluid during isothermal cures at three different temperatures. The match of the results from three different cure cycles suggested that the cure shrinkage is only a function of degree of cure regardless of time and temperature.

Final thickness of composite laminates is strongly related to consolidation of laminates during autoclave processing. Loos and Springer [26] measured the temperature distribution in and the resin flow out of composites constructed from Hercules AS/3501-6 graphite epoxy prepreg tape. Gutowski et al. [27] performed consolidation experiments conducted on special prepregs made of constant viscosity oils and aligned graphite fibers. Measurements of the deformation behavior of the fibers in the "drained" state (oil impregnated, but zero pressure in the oil) revealed that, the fiber network could be modelled as a nonlinear elastic network, and a model based on bending beam behavior was shown to accurately fit the data.

Poursartip and Hubert [28] determined the fibre bed compaction curve directly for AS4/3501-6 composite prepreg. The unidirectional composite specimen was used loaded in the through-thickness direction, which was the main deformation mode of

the fibre bed. A uniaxial testing condition was obtained by preventing the distortion in the transverse direction by the mould walls. The compaction curve of the fibre bed was extracted from the measured displacement and applied load. They [28] also studied the compaction of composite angle laminates. Two types of material, low viscosity AS4/3501-6 and high viscosity AS4/8552 composites, were used as specimens. The low resin viscosity laminates exhibited more resin loss compared to laminates of high resin viscosity. The fibre volume fraction measured in the through-the-thickness and in the longitudinal direction confirmed that under bleed conditions, net percolation of the resin occurs from the tool to the bleeder. Under no-bleed conditions, a small amount of internal percolation could be observed from the corner to the flat section of the angle.

Garstka et al. [2] measured in situ the through-the-thickness strains during processing of AS4/8552. The thermal expansion during the heating stages, the laminate consolidation throughout the cure process, and the cure shrinkage were studied. The tests were performed on $45\text{mm}\times 45\text{mm}\times 4\text{mm}$ samples, for both unidirectional and cross-ply laminates. A ply pull-out technique was used to determine the position of the gel point of the AS4/8552 composite system for various curing temperatures. The relationship between the chemical shrinkage and the degree of cure was deduced from a cure kinetics model. The relative contributions of cure shrinkage, thermal expansion and consolidation to the through-the-thickness strain were distinguished. The through-the-thickness coefficients of thermal expansion for the cross-ply laminate in the liquid and rubbery states were calculated from the average slopes of the plots before and after gelation, and found to be $373\times 10^{-6}\text{ }^{\circ}\text{C}^{-1}$ and $202\times 10^{-6}\text{ }^{\circ}\text{C}^{-1}$, respectively.

The average through-the-thickness strains between gelation and vitrification for samples cured according to the MRCC (Manufacturer's Recommended Cure Cycle) were found to be 0.48% for unidirectional and 0.98% for cross-ply laminates, respectively. Since gelation took place on the second temperature ramp up to the final cure temperature where vitrification occurred, this through-the-thickness strain includes a small component of thermal strain as well as cure shrinkage.

1.2. PROBLEM STATEMENT

The Curing of an epoxy prepreg is a key step in the fabrication of fiber-reinforced thermoset composites. The product quality of composites is controlled to a great extent by the cure cycle parameters such as time, temperature, pressure, and their combination. The epoxy is molded to the shape of final structure and cured by the application of heat. The application of heat can involve different isothermal and dynamic cure cycles which directly generates the mechanical properties of the product.

The curing process optimization and the final product quality require the information of cure kinetics and the physical properties of the epoxy in detail. The right techniques of the process could give better properties. Therefore, the modeling of the cure kinetics is a crucial topic. In this work, two problems will be dealt with; cure kinetics modeling and cure shrinkage measurements.

For the cure kinetic modeling, two types of experiments will be performed to obtain required parameters. The dynamic and isothermal experiments will be performed separately by means of DSC. During the curing reaction, the heat is released, so it is an exothermic process. The heat of the curing reaction is calculated from the area under the heat flow vs. time curve.

The released heat flow measured by DSC is related to degree of cure (α) which is calculated either by the residual heat or by the heat of reaction at a particular time. The published models about the cure kinetics cannot satisfactorily describe the whole process, and a new model of the cure process should be proposed.

Manufacturing of composite materials is a time-consuming and expensive task. While producing a new product, there can be shape distortions which are undesired by producers. These distortions stem from the nature of the curing process. During the cure cycle, the material changes from rubbery to glassy state and attains different properties. Hence, there are residual stresses which are the stresses that remains after the cause of stress is removed. In composites, curing leads to stresses inside the mate-

rial. When the heat is removed, the residual stresses which can cause shape distortions may remain in the part. CTE is also a distinctive property to understand the distortions that may remain in the part. The prepreg consists of two main components; fibers and resin. The fibers have very low CTE along their length. Therefore, in the fiber direction in the composites there cannot be any critical distortions. However, the resin has a higher CTE and can lead to some distortions due to the temperature changes. The incompatibility between the CTEs in different directions on the same material leads to the residual stresses which can affect the material standards and can also contribute to the growth of the failures, such as warpage, cracks, etc.

In brief, the residual stress mainly stems from the resistance of the fibers to the resin not to shrink in the fiber direction. According to the low CTE of fibers and the higher CTE of resin, the major cure shrinkage exists along through-the-thickness direction. The prediction of cure characteristics of the material on thermal process is a necessity for the output quality. The cure shrinkage experiments were usually performed by the researchers using TMA (Thermo Mechanical Analyser) which is appropriate for very small specimens. In the study reported here a different technique was developed to measure the through-thickness strain in the AS4/8552 composite system using a DMA. DMA is a conventional testing equipment and can be used for bigger specimen than TMA's. The technique captures the through-the-thickness thermal expansion during the heating stages. The laminate consolidation throughout the cure process, the cure shrinkage, coefficient of thermal expansion, and the glass transition temperature can be found by the sensitive measurements of DMA. The shrinkage occurring after the point of gelation will be emphasised. The relationship between chemical shrinkage and degree of cure will be deduced from a cure kinetics model of the 8552 resin. In spite of having high displacement sensitivity, TMA (Thermomechanical Analyser) has physical limitations of about the specimen size. But, DMA is highly sensitive to both flow and glass transitions at all states of cure and can perform macro scale measurements. Therefore, DMA is more convenient to test the thermal and cure shrinkage strains of composites.

The specific objectives of the research are as follows:

- To perform dynamic and isothermal experiments using DSC.
- To develop a new model using the measurements of dynamic experiments.
- To compare the results of isothermal experiments and the predictions of the new model by focusing on the degree of cure concept.
- To measure the glass transition temperature, the residual heats, the degree of cure values for various curing schedules.
- To measure the thermal and cure shrinkage strains of the isothermally precured unidirectional and cross-ply samples by using DMA.
- To calculate the coefficient of thermal expansion, the glass transition temperature, and the cure shrinkage values for the unidirectional and cross-ply samples.
- To compare the T_g values obtained by DSC and DMA samples.
- To explore the cure shrinkage strains during the Manufacturer's Recommended Cure Cycle (MRCC).

MRCC is shown in Figure 1.4. The MRCC consists of a first ramp of $2^\circ\text{C}/\text{min}$ up to 120°C and a first hold at 120°C for 60 min, a second ramp of $2^\circ\text{C}/\text{min}$ up to 180°C and a second hold at 180°C for 120 min.

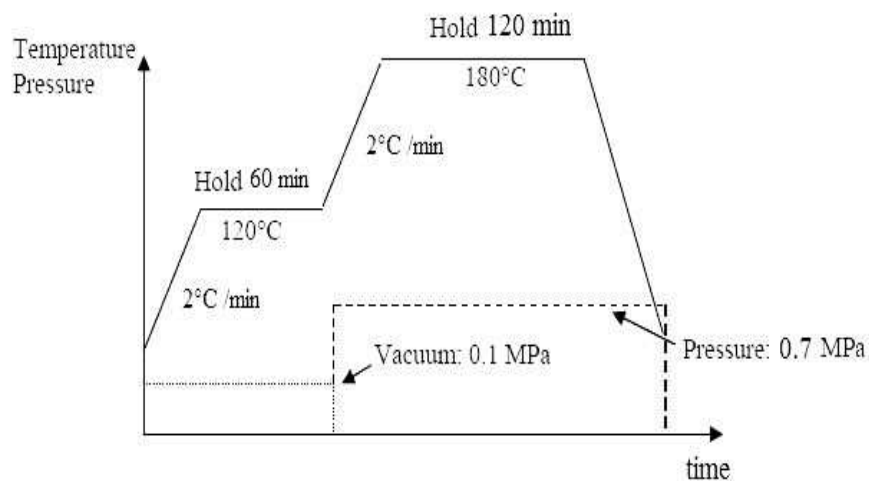


Figure 1.4. Manufacturer's Recommended Cure Cycle

2. EXPERIMENTAL

2.1. DSC EXPERIMENTS

2.1.1. Experimental Material

The prepreg used in this study is a unidirectional carbon/epoxy AS4-8552. Pieces of the prepreg between 5 and 8 mg are used in DSC experiments. This material is an amine cured multifunctional epoxy resin system. The specifications are below in Table 2.1[29]

Table 2.1. Properties of AS4/8552

Carbon fiber areal weight	137 g/m ²
Amount of resin and curing agent	33 wt %

2.1.2. Testing Equipment

2.1.2.1. DSC. A DSC Q200 produced by TA Instruments was used to perform the dynamic and isothermal experiments. The machine mainly includes a sample holder and a reference holder, temperature controller, and a furnace.

Samples are prepared from the prepreg pieces. The pieces were weighed and the mass data were recorded. Small prepreg pieces were cut by a paper punch, put into a standard DSC aluminum pan, and then they were closed by aluminum covers. The reference was an empty aluminum pan with cover. Nitrogen was used as purging gas with flux of 50ml/min. Liquid nitrogen was used as a cooling fluid.

The cure of a resin such as 8552 results in the generation of heat, because low molecular weight monomers are converted into a highly cross-linked polymeric structure. The cure reactions is usually described by the degree of cure, "α", which is

quantified as the fraction of heat generated to that point relative to the total heat generated through the complete cure. The value of alpha can easily be determined using standard heat flow measurements on a DSC by integrating the exothermic DSC peak. The degree of cure of the samples can be found from the residual heat of reaction, H_R and ultimate heat of reaction, H_U using the formula:

$$\alpha = 1 - \frac{H_L}{H_U} \quad (2.1)$$

DSC experiments were performed on the Modulated DSC (MDSC) mode under dynamic and isothermal conditions to provide a database for calculating parameters in model equations in order to describe cure kinetics over a wide range of different conditions. During the experiments the modulation amplitude was $\pm 0.5^\circ\text{C}$. Temperature modulation is used to separate the irreversible heat flow that is related to the cure reaction and reversible heat flow related to the heat capacity of the samples.

2.1.3. Procedure

Dynamic experiments were performed by heating from -35 to 300°C at 1, 2, 3, 4 and $5^\circ\text{C}/\text{min}$. Isothermal experiments were performed by heating from 25°C to 120°C , 140°C , 160°C , 180°C at $5^\circ\text{C}/\text{min}$, then holding at the specified temperature; at 120°C for 360 min., at 140°C for 240 min, at 160°C for 180 min, at 180°C for 120 min. After the isothermal run, the samples were cooled 50°C below the isothermal hold temperature and reheated to 300°C at $5^\circ\text{C}/\text{min}$. All experiments were performed by modulation of temperature of $\pm 0.5^\circ\text{C}$. Mass of prepreg samples that were used in the experiments for each of the dynamic and isothermal cycles are in Table 2.2 and 2.3.

The experiments are completed and the data below are collected for the dynamic and isothermal experiments;

- time
- temperature
- non-reversible heat flow

- reversible heat flow
- non-reversible heat capacity
- reversible heat capacity

The instrument records the heat flow change with respect to the cure time based on the sample size. For the purpose of comparison, the heat flow for each run has been normalized to one gram of sample.

Table 2.2. Prepreg sample mass for dynamic experiments

Heating rate (K/min)	Sample mass (mg)
1	7.20
2	6.10
3	6.50
4	6.10
5	5.30

Table 2.3. Prepreg sample mass for isothermal experiments

Isothermal temperature (°C)	Sample mass (mg)
120	6.50
140	6.70
160	6.60
180	5.90

2.2. DMA EXPERIMENTS

2.2.1. Experimental Material

2.2.1.1. Sample preparations. Ten samples were prepared for DMA experiments; five unidirectional (UD), five cross-ply (XP). Prepreg tape has a thickness of 0.184 mm and has carbon fibers running in one direction.

For each specimen the prepreg tapes were cut into 26 pieces which had the dimensions of 60×60 mm and laid-up to UD and XP samples.

A home-made autoclave were used to cure the specimens. It has a rectangular prism shape and removable front, back and upper covers with a compressor inlet. Its one side has a vacuum inlet and it is heated by resistance coils at bottom and sides. To control the temperature thermocouples are replaced to the material that will be cured and thermocouples are connected to a PID control unit which has various program selections such as heating rate, isothermal hold duration etc...

Afterwards a pair of UD and XP samples was carefully laid-up into the mold that was produced from rubber. Then, plies were covered up by aluminum plates with dimensions of 60×60 mm, too. The contact faces of aluminum with composite were covered by peel plies which were teflon coated glass woven fabrics that were generally applied as the last material in the composite lay-up sequence and designed to make a textured surface on the produced composite parts. On this system, a breather fabric was laid-up to allow the vacuum to be equally distributed. The fabric also provides a path for entrapped air to leave the laminates.

A vacuum bag with a vacuum inlet was applied to the whole lay-up with a sealant. The vacuum pump were started and the thermocouples were replaced onto appropriate places.

Then all sides of the autoclave were screwed tightly. The compressor pump were run at 7 bar pressure.

After all these preparations the PID temperature controllers were programmed and curing was started. At curing stages firstly temperature program was started from the room temperature, increased to 120°C by 2°C/min, and kept at 120°C for 1 hour. Then the temperature was reached to desired temperature for each experiments by 2°C/min and kept for desired time interval at this temperature, can be shown in Table 2.4.

For the last two composites which includes a UD and a XP laminates, the procedure were stopped after one hour isothermal hold at 120°C and the temperature of the composite were decreased to room temperature. These fabricated composites were cut into 20×20 mm parts by a precision cutter supported by liquid coolant. To overcome the temperature gradient between material and DMA’s heat measurements, the composites were drilled a 2mm diameter hole at one of the corners, which could accommodate the DMA’s control thermocouple.

Table 2.4. Time intervals for isothermal experiments

Temperature (°C)	120	140	160	180
Holding time (hours)	6	4	3	2

2.2.2. Testing Equipment

2.2.2.1. DMA. A Differential Mechanical Analyzer Q800 from TA Instruments was used to perform the dynamic and isothermal experiments. A compression clamp is used in the machine mainly includes two clamps (bottom clamp is fixed, the upper clamp can move), a thermocouple, and a furnace.

DMA was used in compression mode. The sample were placed onto the fixed clamp and the moving clamp was pressed until touching the sample. Moving clamp applies a very small force on sample not to allow disengagement of the sample from the clamp, so measures the sample’s dimensional changes as displacement. Nitrogen was used as purging gas with flux of 50ml/min. Also liquid nitrogen was used to get a controlled cooling.

Before the DMA experiments, a temperature calibration performed using a thermocouple which is touching the sample directly. The results showed that there is a considerable difference between the temperatures of the thermocouple touching to the sample and the DMA equipment’s control thermocouple.

A major aspect regarding the accuracy of the experiments performed in a DMA

is the precise knowledge of the sample temperature as the physical properties are monitored. It must be pointed out that it is not possible to attribute a single temperature to the sample because of its own resistance, especially if it is a bad heat conductor, so in practice there are distinct temperatures at distinct points of the sample and the designation "true or real sample temperature" that appears in literature is in fact an average sample temperature. In DMA, the temperature sensor is close to but separated by a gas gap from the sample. Differences between the sample temperature and the temperature read by the sensor are due to different factors that include the set of thermal resistances (sample, accessories, purge gas), the heat fluxes inside the furnace and the accuracy of the sensor reading.

In order to avoid the thermal lag between the specimen and the control thermocouple, the control thermocouple of the DMA equipment is placed inside a hole drilled at the corner of the specimen to directly measure the temperature of the specimen (seen in Figure 2.1).

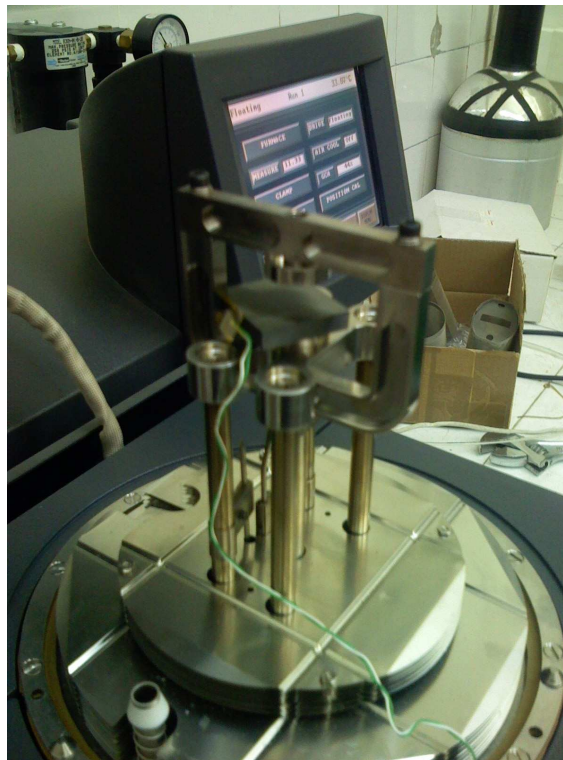


Figure 2.1. Specimen on compression clamps used in the DMA

2.2.3. Tests

Eight samples (four of them were unidirectional, others were cross-ply), that are produced according to the procedure given in Table 2.4, were heated from the room temperature up to 250°C and cooled back to room temperature at a rate of 2°C/min. Also, the empty clamp was tested according to the same procedure in order to provide a baseline to be subtracted from the response of the composite samples. The last two samples, which were autoclaved for one hour at 120°C, were heated from room temperature up to 180°C at 2°C/min and held by two hours (the empty clamp was tested according to the same procedure, too). Two additional tests (one for UD, one for XP) were performed with the fully cured samples which were tested before.

3. MODELING

Producers need a convenient reaction model to manufacture products with specific properties and also to save time and capital. The reaction of the thermoset materials is complicated because of the close relations between the temperature and the material phase. In the modeling, the main purpose is to calculate the degree of cure value for any curing schedule.

3.1. Degree of Cure

The curing of epoxy prepreps involves a phase transition from rubbery to glassy state. This chemical reaction is an exothermic reaction and irreversible. At the glass transition point, the matrix loses its rubbery form and begins to generate heat. The generated heat at a specific time is related to the degree of cure at that time. The degree of cure increases as the heat of reaction increases; so they are proportional to each other. A completely cured material has a degree of cure of unity. The general method to calculate the degree of cure is the difference between unity and the ratio of residual heat to the total heat of reaction.

$$\alpha = 1 - \frac{H_r}{H_u} \quad (3.1)$$

where α is the degree of cure, H_r is the residual heat of reaction, and H_u is the total or ultimate heat of reaction. The effective method is to use the ratio of an instantaneous value of heat of reaction to the total heat of reaction.

$$\alpha = \frac{H_t}{H_u} \quad (3.2)$$

where H_t is the partial heat of reaction at time t .

3.2. Cure Rate

For modeling different techniques could be used. The first order, the n^{th} order, and the autocatalytic reaction models are the basic ones. The experimental instrument (DSC) provides the measurements of cure rate and the computer based data analysis programs determine the kinetic information. The basic assumption to characterize the curing kinetics of epoxy can be obtained by the differentiating Eq.3.2:

$$\frac{dH}{dt} = \frac{d\alpha}{dt} H_u \quad (3.3)$$

$d\alpha/dt$ is the reaction or cure rate. If the diffusion of chemical species is neglected, the degree of cure of the material can be calculated in the following way

$$\alpha = \int \left(\frac{d\alpha}{dt} \right) dt \quad (3.4)$$

The dependence of the cure rate on the temperature and on the degree of cure must be known. The dependence can be expressed as

$$\frac{d\alpha}{dt} = f(T, \alpha) \quad (3.5)$$

The functional relationship in Eq.3.5 and the value of the heat of reaction can be determined experimentally. The heat of reaction, the rate of cure, and the degree of cure can be measured with a DSC. The isothermal heat of reaction H_T is defined as the total amount of heat generated from time $t=0$ until no evidence is found of further reactions at a constant temperature. The ultimate heat of reaction H_u is the amount of

heat generated during dynamic scanning until the completion of the chemical reactions.

The ultimate heat of reaction H_u is a constant, and is independent of the heating rate. H_T depends on the temperature.

The ultimate heat of reaction H_u is determined directly from the results of dynamic scanning measurements. The value of H_T can be determined from the results of the isothermal or dynamic scanning measurements.

The rate of cure is a parameter proportional to the rate of the heat release at a constant temperature T

$$\frac{d\alpha}{dt} = \frac{1}{H_u} \left(\frac{dQ}{dt} \right)_T \quad (3.6)$$

dQ/dt is heat flow rate with respect to time.

3.3. Proposed Model

α and $d\alpha/dt$ are two of the parameters of most interest in cure process simulations. In order to represent them, Eq.3.6 is rewritten in the form

$$\frac{d\alpha}{dt} = \frac{H_T}{H_u} \frac{1}{H_T} \left(\frac{dQ}{dt} \right)_T \quad (3.7)$$

or

$$\frac{d\alpha}{dt} = \frac{H_T}{H_u} \frac{d\alpha_i}{dt} \quad (3.8)$$

where $d\alpha_i/dt$ is an isothermal rate of cure defined as

$$\frac{d\alpha_i}{dt} = \frac{1}{H_T} \left(\frac{dQ}{dt} \right)_T \quad (3.9)$$

The degree of cure is obtained by integrating Eq.3.8

$$\alpha = \int \left(\frac{H_T}{H_u} \right) \frac{d\alpha_i}{dt} dt \quad (3.10)$$

The ratio of H_T/H_u is obtained by a least square curve fit to the experimental data of H_T/H_u versus temperature. Thus, $d\alpha/dt$ and α can be calculated at any temperature from Eqs.3.8 and 3.10. In our model the following form for $d\alpha/dt$ as proposed by Kolbeck et al.[30] is used.

$$\frac{d\alpha}{dt} = k_1\alpha^{a_1}(1 - \alpha)^{n_1} + k_2\alpha^{a_2}(1 - \alpha)^{n_2} \quad (3.11)$$

This form is the main equation of our model and a modified version of the Sourour-Kamal equation [31] which means a single-step parallel reaction (as in Figure 3.1) with diffusion control of the autocatalytic model for the cure reaction. The reason for using a single-step parallel reaction is the shoulder in the nonreversible heat flow curves in the Figure 4.1. The shoulder represents the peak of the second reaction.

The exponents a_1 , n_1 , a_2 , and n_2 are the parameters, independent of temperature. k_1 and k_2 are called effective rate constants.

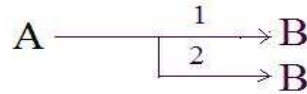


Figure 3.1. Single-step parallel reaction model

The diffusion effect is incorporated into the model by allowing the reciprocal of the effective rate constant to be the sum of the reciprocals of the chemical and diffusion rate constants by Rabinowitch equation [13]:

$$\frac{1}{k_{1,2}} = \left(\frac{1}{k_{1,2}^{chem}} \right) + \left(\frac{1}{k_{1,2}^{diff}} \right) \quad (3.12)$$

The chemical rate constant, which depend on the temperature, is described in the form of the Arrhenius equation:

$$k_{1,2}^{chem} = A_{1,2} \exp \frac{-\Delta E_{1,2}}{RT} \quad (3.13)$$

A_1 and A_2 are the pre-exponential factors. ΔE_1 and ΔE_2 are the activation energies, R is the universal gas constant, and T is the absolute temperatures in degrees Kelvin.

A modified WLF (Williams Landel Ferry) equation was used as proposed by Wise et al.[14]

$$k_{1,2}^{diff} = K_{1,2}^{diff} \exp \frac{C_1 * (T - T_g)}{C_2 + |T - T_g|} \quad (3.14)$$

K_1^{diff} , K_2^{diff} , C_1 , and C_2 are the parameters to be found. The model is build up 12 parameter which are listed in Table 3.1.

Table 3.1. Parameters of the model

Parameters to be found	Reaction orders		Chemical cure rate parameters		Diffusive cure rate parameters	
	Reaction1	a_1	n_1	A_1	E_1	K_1^{diff}
Reaction2	a_2	n_2	A_2	E_2	K_2^{diff}	C_2

The estimated model is studied with the multivariate nonlinear regression analysis using the "Netzsch Kinetics" commercial software. The software has a convenient option of diffusion controlled reaction. To use this option T_g versus the degree of cure function must be loaded before performing a nonlinear least square fit. T_g versus α data is plotted in Figure 3.2. The $T_g(\alpha)$ function is fitted to the equation:

$$T_g(\alpha) = T_g(0) \exp\left(\frac{g_1 \alpha}{g_2 - \alpha}\right) \quad (3.15)$$

$T_g(0)$, g_1 , and g_2 are the constants which are found to be; 2.0434, 0.7820, and 2.2917, respectively.

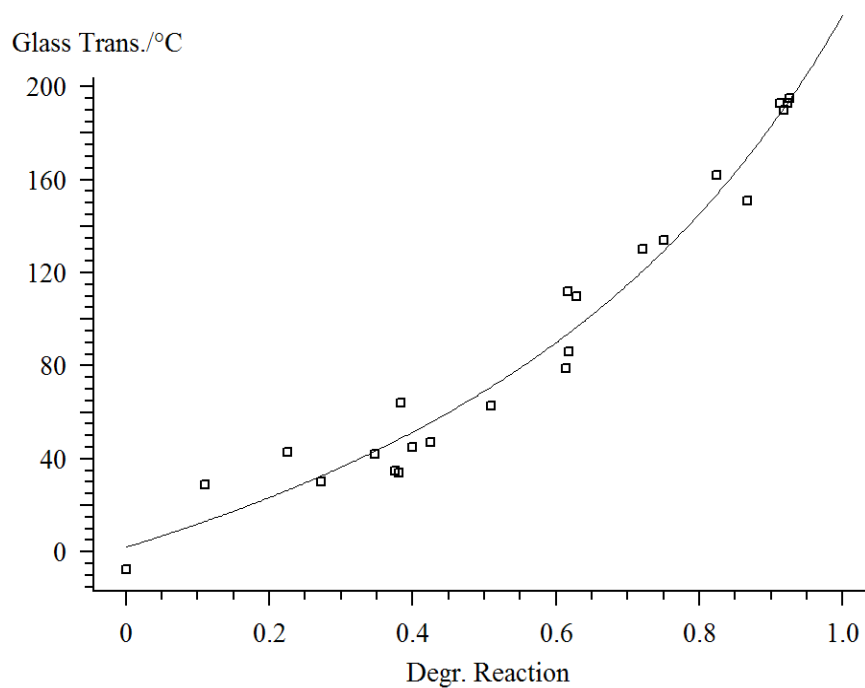


Figure 3.2. The relationship between T_g and α for AS4/8552 composite

4. RESULTS AND DISCUSSION

4.1. DSC STUDY

4.1.1. DSC Dynamic Cure Analysis

The dynamic and isothermal measurements were done to obtain more information about the curing process by DSC which is used in the modulated DSC mode. For dynamic measurements, the samples were scanned from -35 up to 300°C with constant heating rates of 1, 2, 3, 4, and 5°C/min. Figure 4.1 gives the nonreversible heat flow change at the heating rates in the temperature range from -35 up to 300°C. It shows the heat flow changes with temperature. For higher heating rates, the starting and ending points of the reaction shifted to the higher temperatures. Also, exothermal peak temperature increased. In Figure 4.1, two peaks can be seen clearly on the first graph which belongs to the 1°C/min experiment. As the heating rate increased, the peaks overlap. These are assumed to be two separate reactions. The first reaction happens at lower temperatures; the second one at higher temperatures. The heat flow of the second reaction increased when the heating rate is increased.

Figure 4.2 shows the nonreversible heat flow change versus time after a baseline removed. The cure heat of reaction of each experiments were calculated from Figure 4.2 by the integration method. In this method, straight baselines were drawn under the peak of each curve and the areas were integrated (see Figure 4.3).

Table 4.1 gives the calculated total heat of reaction values of uncured samples for each heating rate. The average curing heat of reaction was found to be 186.36 ± 18.74 J/g for the composite with 33wt % resin which corresponds to 559.08 J/g for the pure resin which is close to the values cited in the literature [32][33].

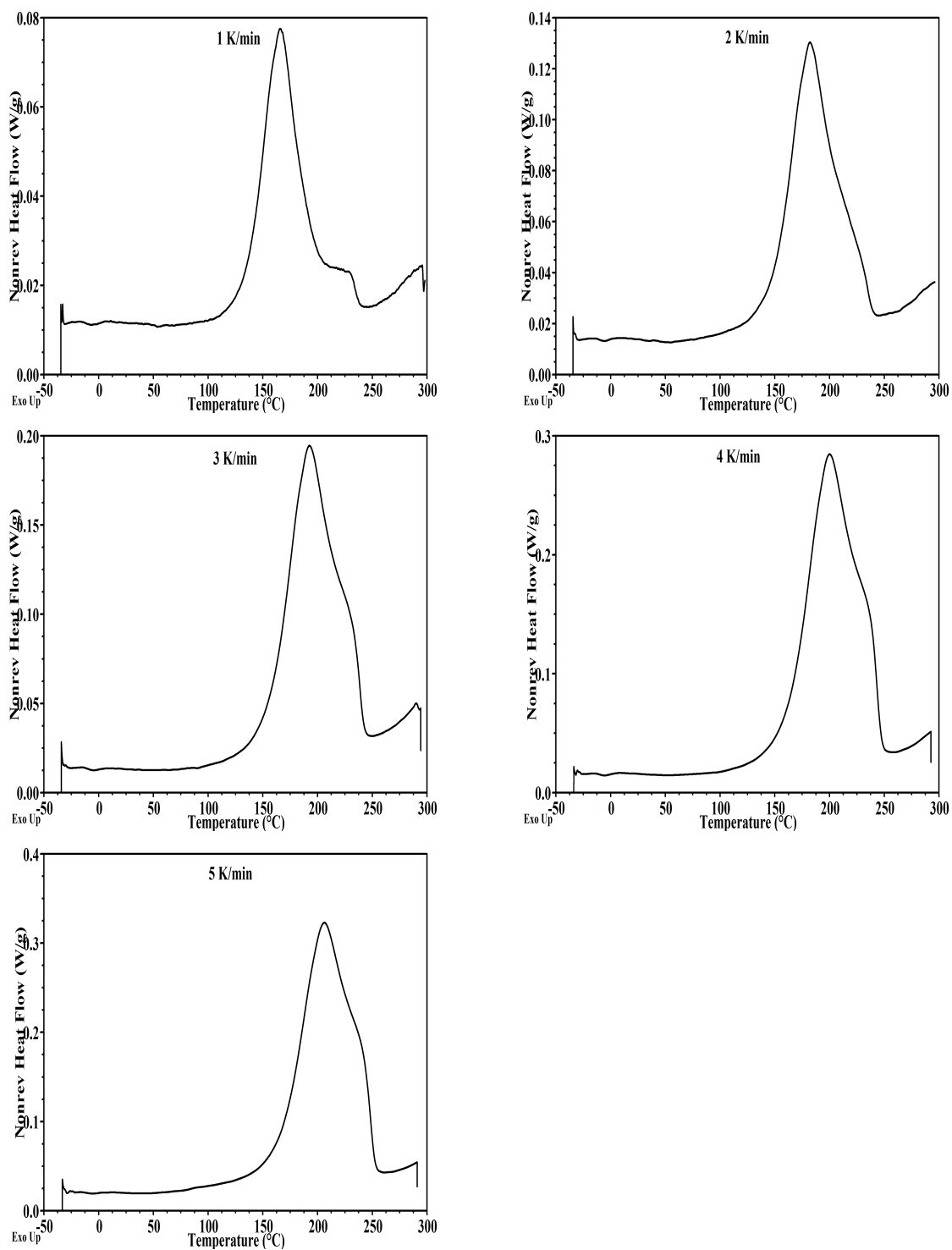


Figure 4.1. Nonreversible heat flow vs. temperature graphs of prepregs cured by 1 ,2 , 3, 4, and 5 K/min dynamic rates

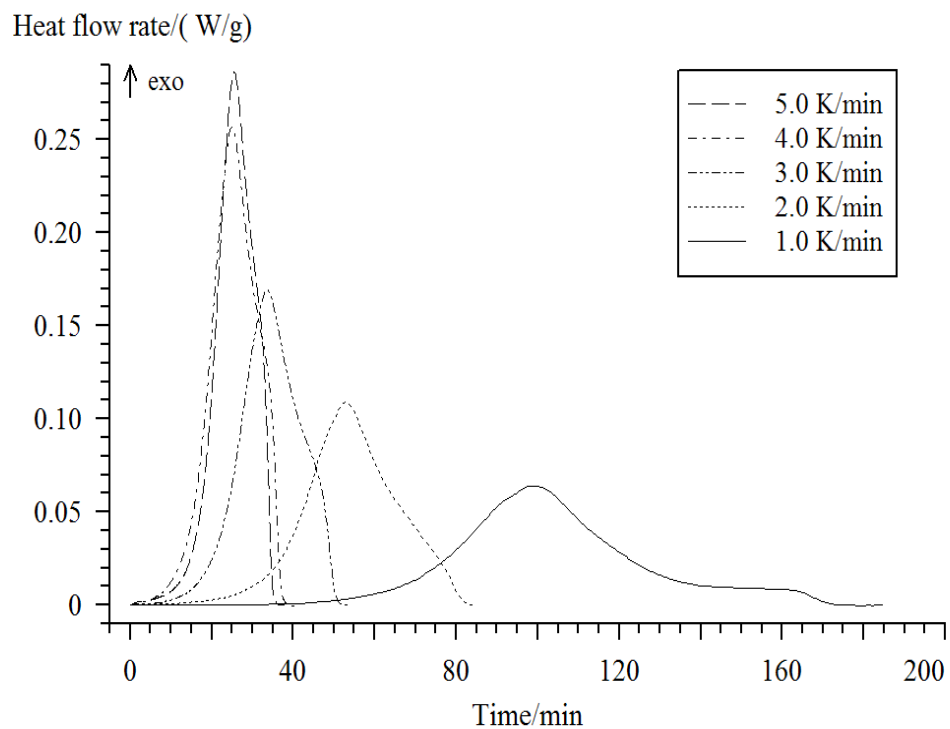


Figure 4.2. Nonreversible heat flow vs. time graphs of prepreps cured by 1, 2, 3, 4, and 5 K/min dynamic rates

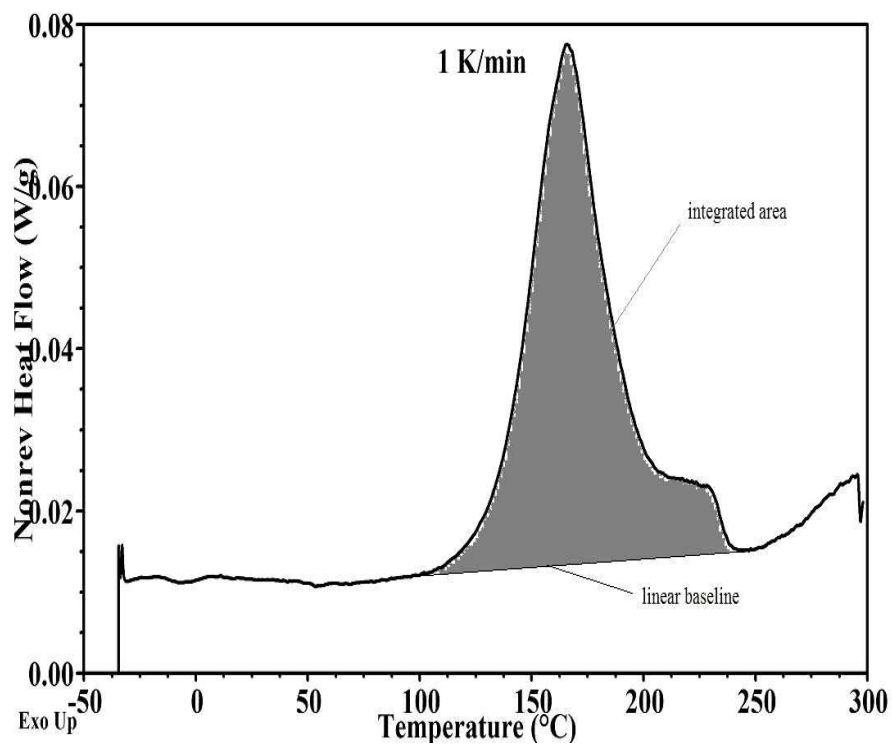


Figure 4.3. Integration method to calculate the curing heat of reaction for 1 K/min dynamic experiment as an example

Table 4.1. Total heat of reaction values for dynamic experiments

Heating rate (K/min)	heat flow of reaction (J/g)
1	196.01
2	213.65
3	181.45
4	167.35
5	172.86
Average total heat flow of reaction	186.36±18.74

4.1.2. Cure Kinetic Modelling

Cure kinetic modeling was carried out using the Software "NETZSCH Thermokinetics". The diffusion control option is applied for all reactions and the T_g versus α data, which is plotted in Figure 3.2, are loaded to the software.

For the fitting of the experimental curves to the model curves, the selection of initial values for the parameters is very important. During the process of nonlinear regression, the sum of the squares of the deviations of the theoretical values from the experimental values, which is called " x^2 ", decreases as the parameters change. The nonlinear regression stops when x^2 values are minimum and the parameters do not change with additional iterations. The values for the parameters thus obtained are the best values for the model to describe the experimental data [9]. Figure 4.4 gives the fitted curves and the experimental curves.

The fitted curves agree well with the experimental data. The parameter values for the model are listed in Table 4.2

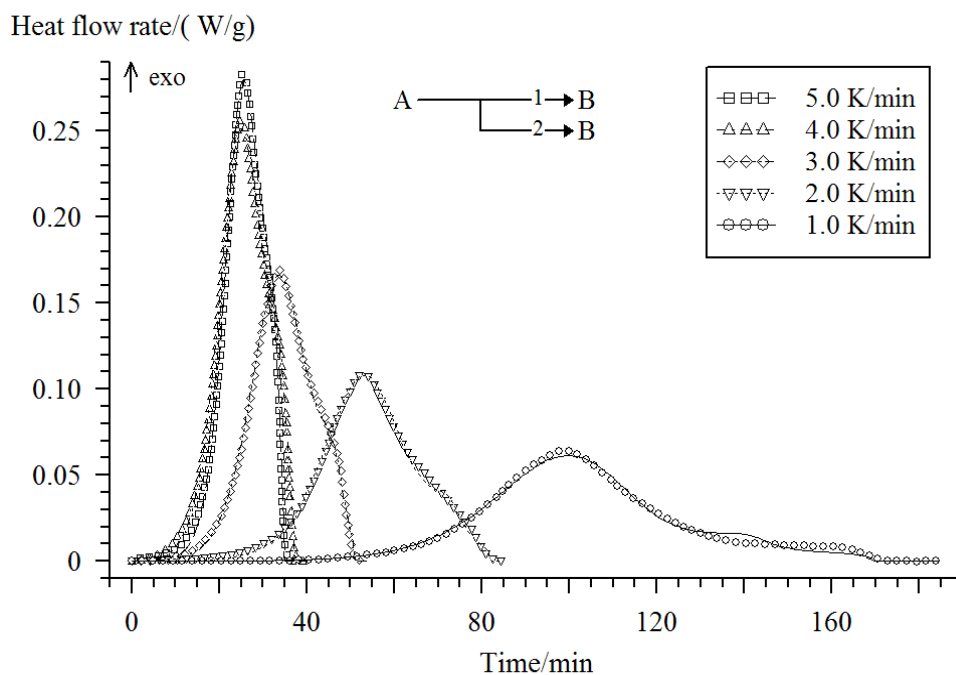


Figure 4.4. Nonreversible heat flow vs. time graph of prepreps cured by 1, 2, 3, 4, and 5 K/min dynamic rates respectively, with model fit shown as continuous curves

Table 4.2. Parameter values of the model; found by the nonlinear regression analysis of the software

Parameter name	Unit	Value
$\log A_1$	s^{-1}	10.6047
E_1	kJ/mol	129.8464
n_1		0.3946
a_1		6.5163E-5
$\log K_{diff1}$	s^{-1}	-4.0229
$\log A_2$	s^{-1}	5.0451
E_2	kJ/mol	66.7952
n_2		1.2783
a_2		0.4535
$\log K_{diff2}$	s^{-1}	-5.0136
C_1		8.2558
C_2	1/K	27.1837

4.1.3. DSC Isothermal Cure Analysis

A series of isothermal measurements were performed, starting from 120°C up to 180°C. The measurement time was set long enough to obtain nearly constant heat flow in the late cure stage, from 120 minutes at 180°C to 360 minutes at 120°C. After the isothermal runs, the samples were cooled to 50°C below the isothermal hold temperature and reheated to 300°C at 5 °C /min. All experiments were performed by modulation of $\pm 0.5^\circ\text{C}$. The heat flow was plotted against cure time for the runs at each cure temperature.

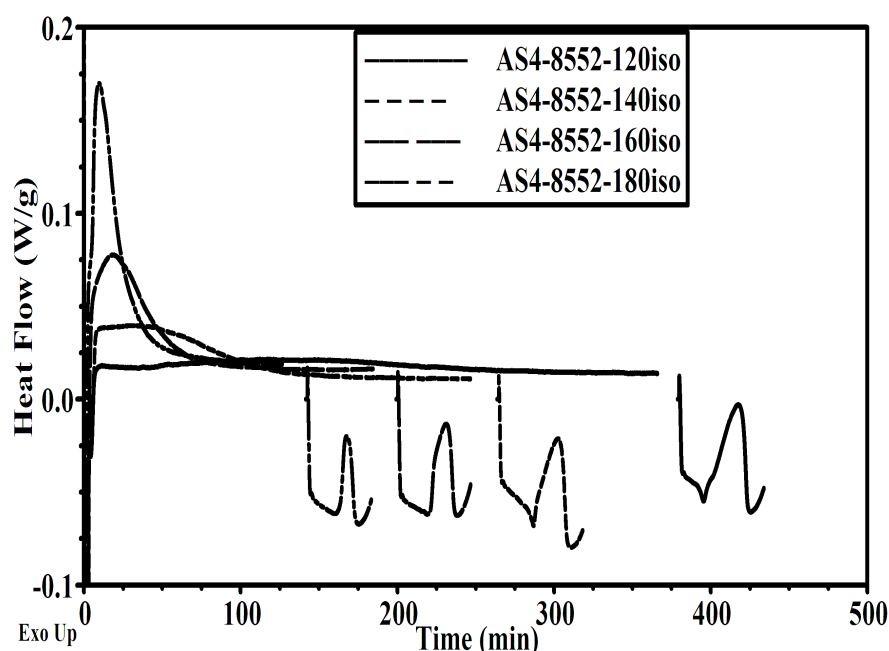


Figure 4.5. Heat flow vs. time graphs of the isothermal experiments; the heats of reaction are the peaks at the left; the residual heats are the peaks at the right

As shown in in Figure 4.5 for the isothermal cure processes at 120°C, 140°C, 160°C, and 180°C, each curve exhibits a peak and finally becomes horizontal. The isothermal cure reaction is almost complete after the heat flow curve becomes horizontal at each cure temperature. Cooling to 50°C below the isothermal hold temperature and heating up to 300°C at 5 °C /min is the second part of the experiments and is performed to measure the residual heat of the isothermally cured materials. The peaks at the right side of the Figure 4.5 represents the residual heats of the samples. In Figures 4.6, 4.7,

4.8 and 4.9 the nonreversible heat and the reversible heat versus temperature graph of the second parts of the isothermal experiments can be seen in detail. These are very important to calculate residual heat, that is a key parameter to find the degree of cure, and the glass transition temperature. T_g can be found either from the step change in the reversible heat flow curve, or from the onset temperature of the reaction which can be measured from the nonreversible heat flow curve.

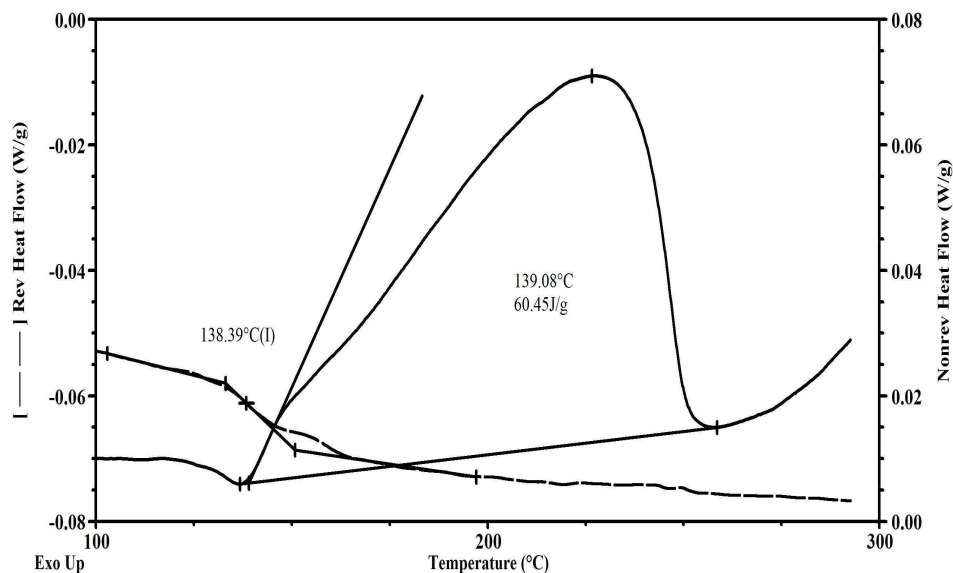


Figure 4.6. Nonreversible and reversible heat flow vs. time graphs during reheating stage of prepregs cured isothermally at 120; T_g value found by reversible heat flow curve; residual heat found by nonreversible heat flow curve

The T_g values found by the two methods were given in Table 4.3. The values measured from the reversible and nonreversible heat flow curves are very close to each other.

Table 4.4 contains the residual heat values found by the baselined integration method. The residual heat of reaction was calculated by integrating the area under the peak with the linear baseline between the onset and ending temperatures of polymerization. As the isothermal temperature increase, the T_g value increases, while the residual heat value decreases.

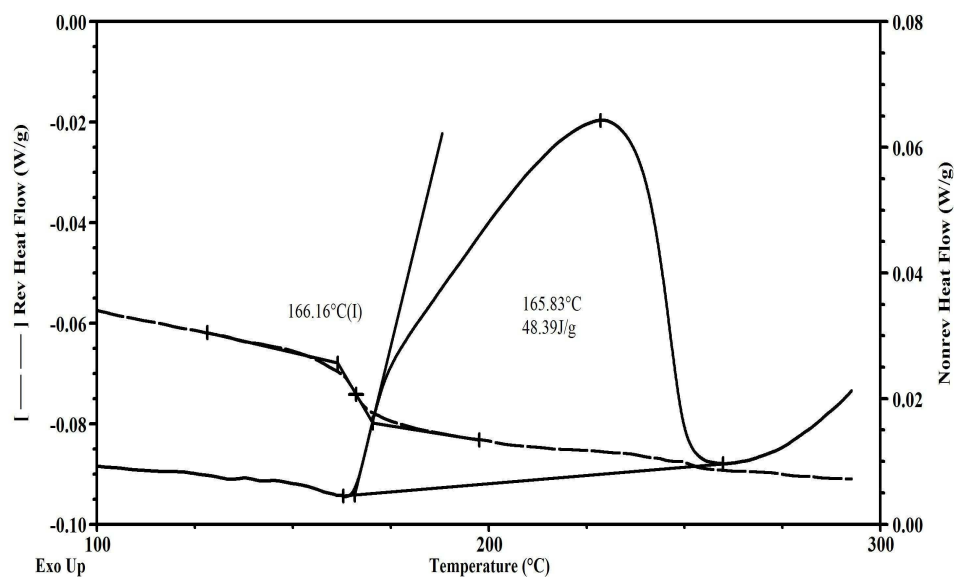


Figure 4.7. Nonreversible and reversible heat flow vs. time graphs during reheating stage of preregs cured isothermally at 140°C; T_g value found by reversible heat flow curve; residual heat found by nonreversible heat flow curve

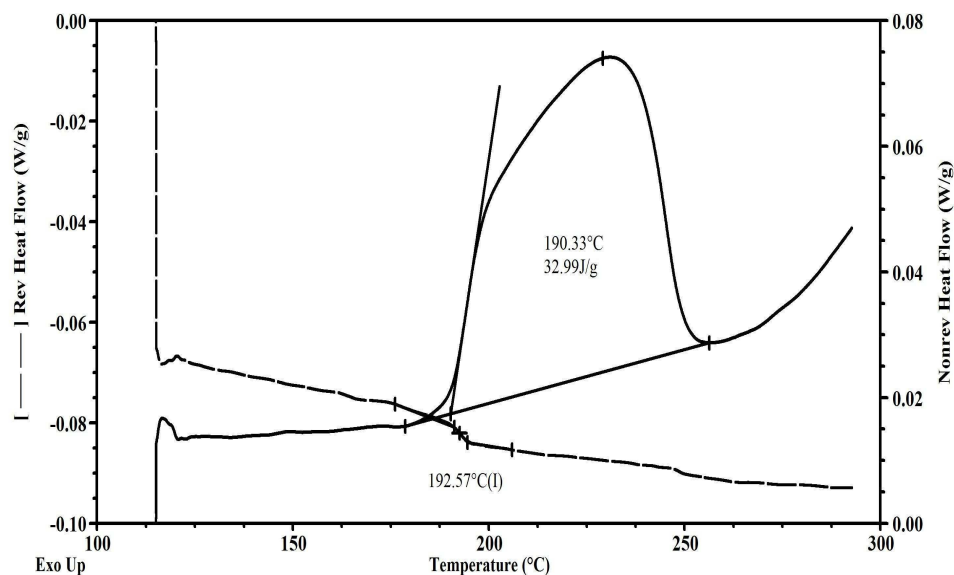


Figure 4.8. Nonreversible and reversible heat flow vs. time graphs during reheating stage of preregs cured isothermally at 160°C; T_g value found by reversible heat flow curve; residual heat found by nonreversible heat flow curve

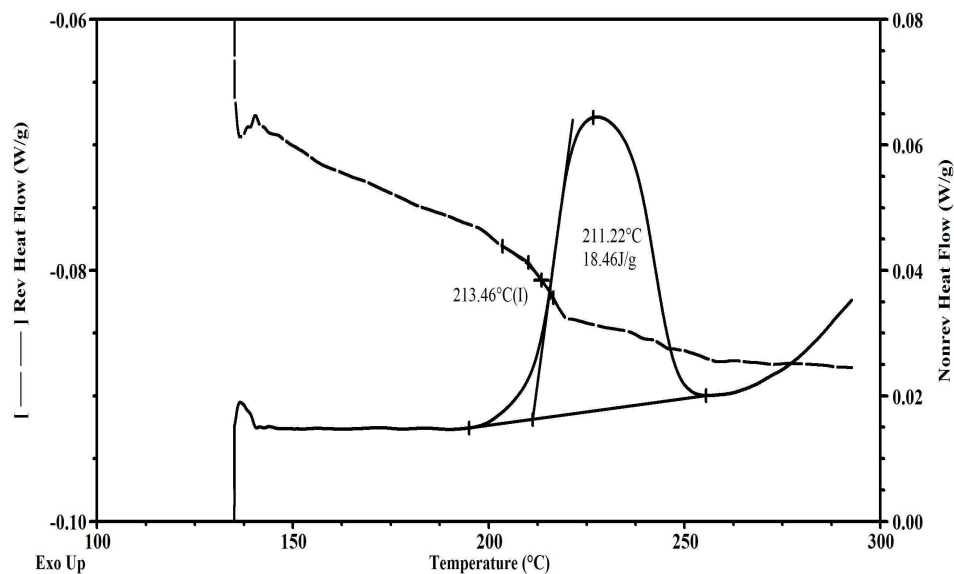


Figure 4.9. Nonreversible and reversible heat flow vs. time graphs during reheating stage of prepregs cured isothermally at 180°C; T_g value found by reversible heat flow curve; residual heat found by nonreversible heat flow curve

Table 4.3. Glass transition temperatures from reversible and nonreversible heat flow measurements of prepreg for isothermal experiments

Isothermal temperature (°C)	Duration of isothermal curing (min)	T_g value measured from	
		Nonreversible heat flow curve (°C)	Reversible heat flow curve (°C)
120	360	139.08	138.39
140	240	165.83	166.16
160	180	190.33	192.57
180	120	211.22	213.44

Table 4.4. Isothermal heat of reaction, residual heat of reaction, measured and predicted degrees of cure, and glass transition temperatures of samples precured isothermally

Isothermal Temperature (°C)	Hold Time (min)	Isothermal Heat (J/g)	Residual Heat (J/g)	Total Heat (J/g)	Predicted α	Measured α	T_g (°C)
120	360	78.38	60.45	169.72	0.692	0.678	138.4
140	240	141.61	48.39	180.84	0.747	0.742	166.1
160	180	138.64	32.99	196.11	0.824	0.823	192.6
180	120	184.73	18.46	213.63	0.892	0.900	214.4

4.1.4. Comparison of Model Predictions and Isothermal Measurements

Based on the kinetic model and the calculated parameters, isothermal DSC signal of the samples can be predicted and compared with the measured signal. Table 4.4 shows the calculated and predicted maximum degree of cure values for the isothermally cured materials. The prediction was performed by using the cure kinetics model developed in this study.

The isothermal heat flows of reaction showed reasonably good agreement with the predictions as; shown in the Figures 4.11 and 4.10. As the model curves fit well to the dynamic experimental curves, the predictions of the model for isothermal part of the study are also satisfying.

Figure 4.12 provides the predicted degree of cure behavior of the isothermal curing. While cured part increasing, the uncured part decreases. One can say that the selected time intervals of the isothermal experiments allow complete curing. After waiting for a certain duration, the reaction cannot proceed any more and a maximum degree of cure is reached.

Based on the cure kinetic model developed in this study, one can also predict the

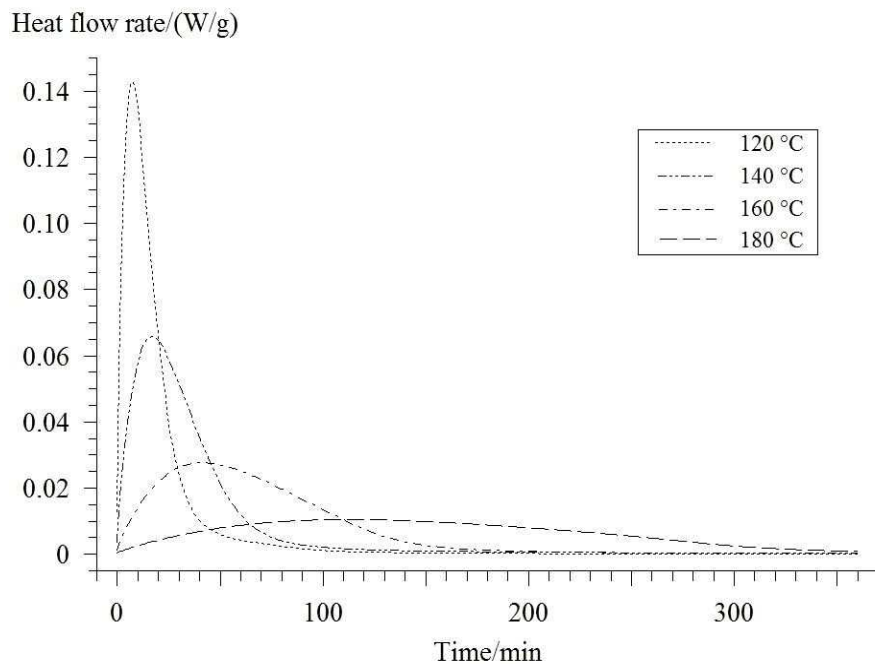


Figure 4.10. Isothermal predictions of the model based on dynamic experiments

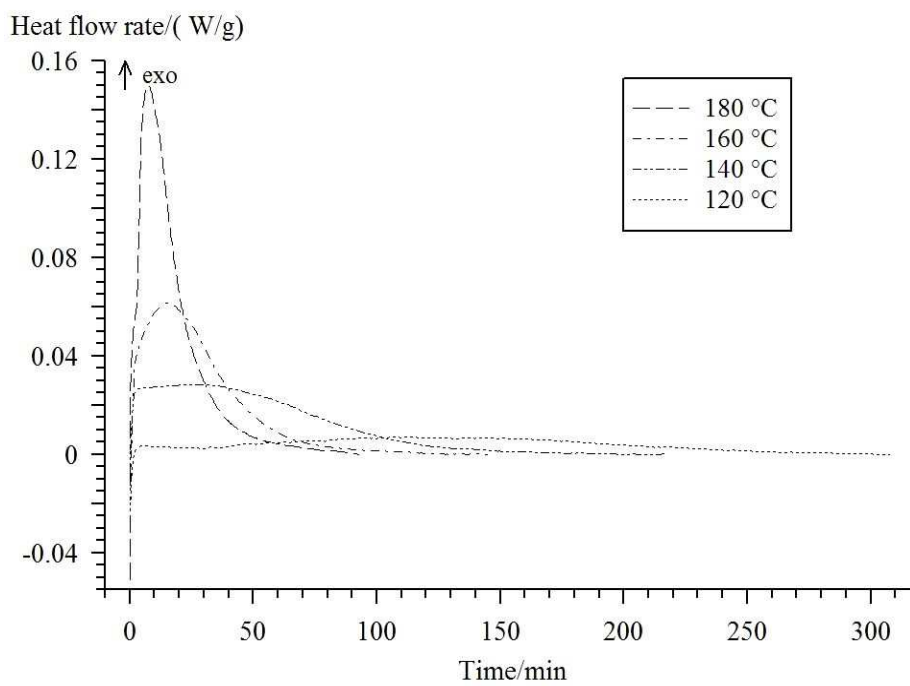


Figure 4.11. Heat flow vs. time graphs of the isothermal experiments

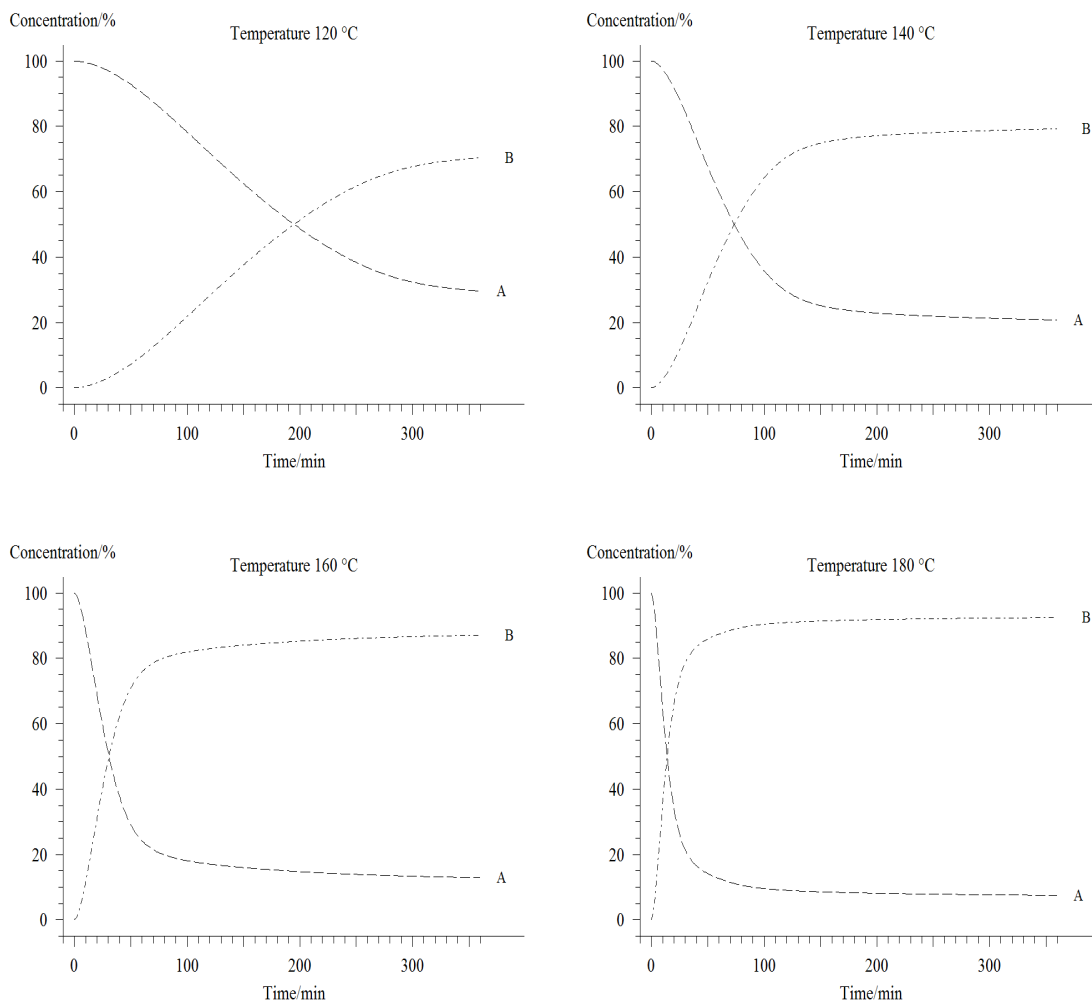


Figure 4.12. Isothermal predictions of the model according to the cure kinetics model; A=uncured part, B=cured part

isothermal conversion fraction (degree of cure) as a function of time at various curing temperatures. Results showed that the calculated cure rate vs. time curves at 120°C, 140°C, 160°C, and 180°C are in good agreement with the experimental data. Figure 4.13 shows the final product vs. time graph of the isothermal prediction of the model.

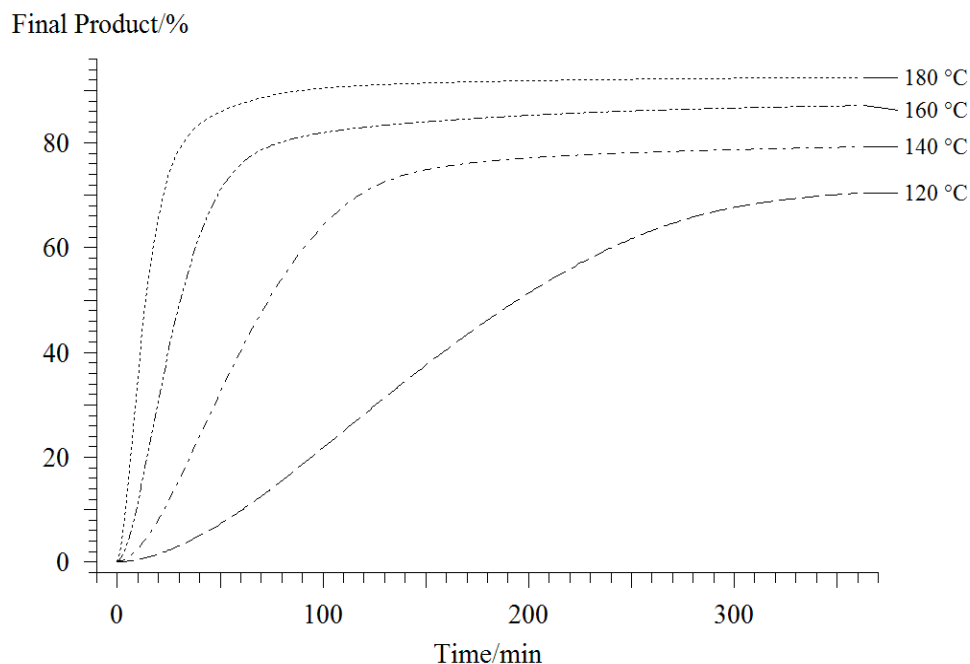


Figure 4.13. Isothermal predictions of the model according to cure kinetics model

4.2. DMA STUDY

4.2.1. Analysis of isothermal results

Eight samples (four unidirectional and four cross-ply) that are produced according to the curing schedule described in Table 2.4, were heated from the room temperature up to 250°C and cooled to room temperature with a heating rate of 2°C/min. The empty clamp of DMA is also subjected to the same thermal cycle and the result of the clamp was subtracted from all of the results of the samples. Figure 4.14 shows the displacement measurements of XP and UD samples precured isothermally for 180°C, together with the thermal response of the empty clamp.

The results for the tests can be shown in Figures 4.15, 4.16, 4.17, and 4.18. One

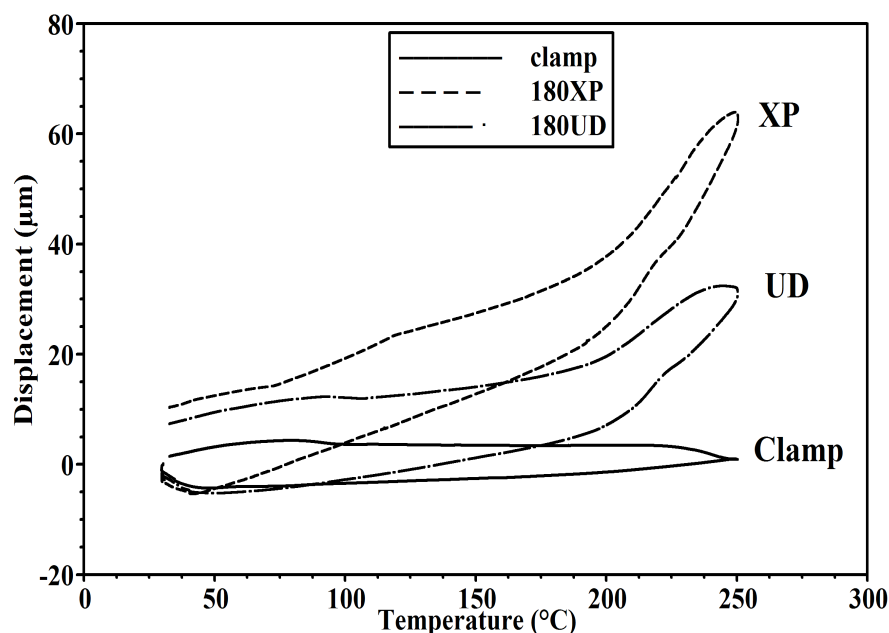


Figure 4.14. Displacement vs. temperature graphs of heating and cooling cycle of XP and UD samples precured isothermally for 180°C, together with the thermal response of the empty clamp

can see that the XP samples strain values are always higher than the UD's'.

From the measurements, T_g values were calculated for heating and cooling stages separately. During heating; the first kink gives the T_g value of the partially cured sample, the second kink reflects the onset of the curing reaction whereas the third kink is the end. During cooling, the only kink gives the T_g of fully cured sample (can be seen in Figure 4.20 as an example, more curves are given in Appendix A). The T_g values are listed in Table 4.10. After the curing, T_g values became higher than the T_g values of the precured samples. Also, as the isothermal temperature at which the samples are precured, increases, the T_g values increase. The cooling parts of the experiments have almost same values of T_g . Here "fully cured" means that all possible cross links are formed as determined by the stoichiometry of the monomers and curing agent. Since here is long flexible segments between crosslink sites are present, the freezing of the motion of these segments causes glass transition during cooling.

Another important parameter in the study is the CTE value. To calculate this value the graphs were analyzed in four regions: The first one is the heating before the

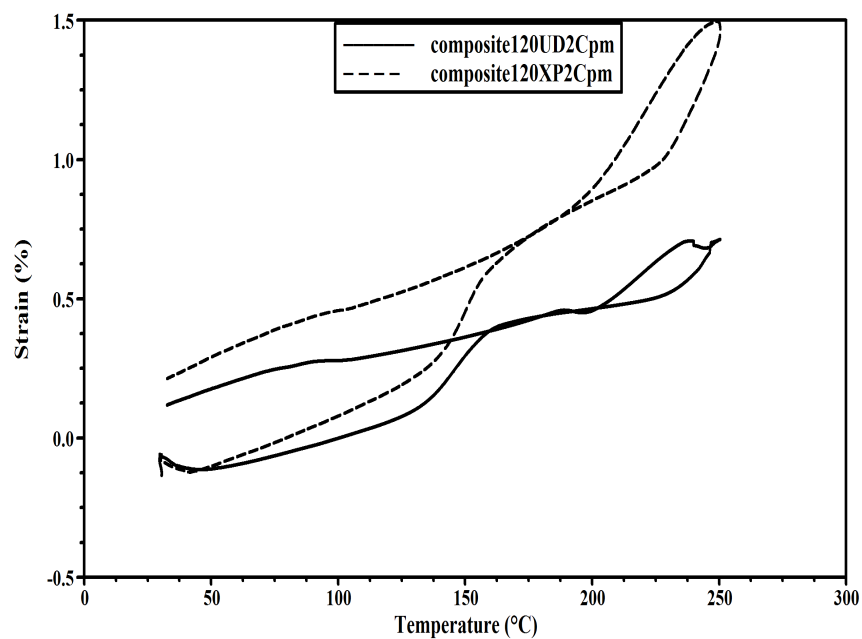


Figure 4.15. Strain vs. temperature graphs of cross-ply and unidirectional samples precured isothermally for 120°C; including both heating and cooling stages

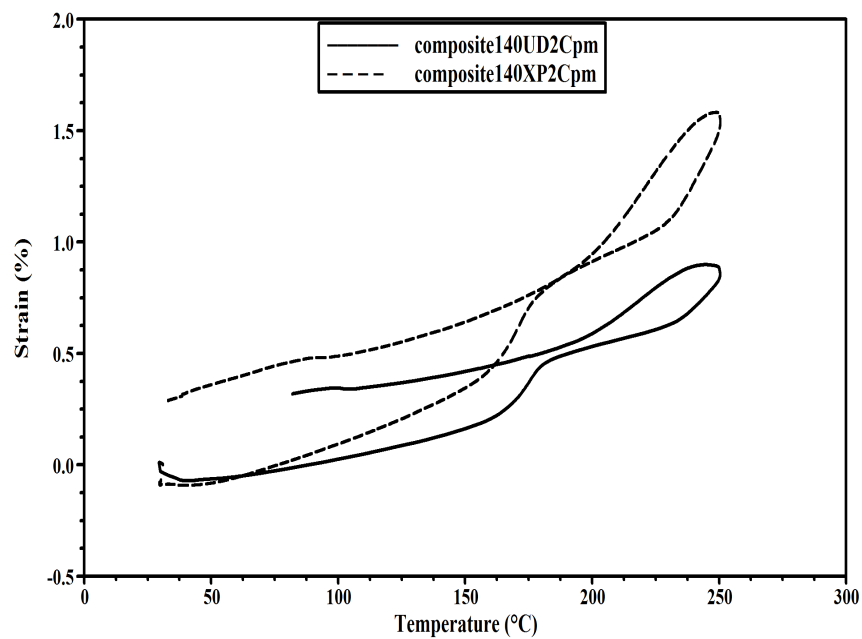


Figure 4.16. Strain vs. temperature graphs of cross-ply and unidirectional samples precured isothermally for 140°C; including both heating and cooling stages

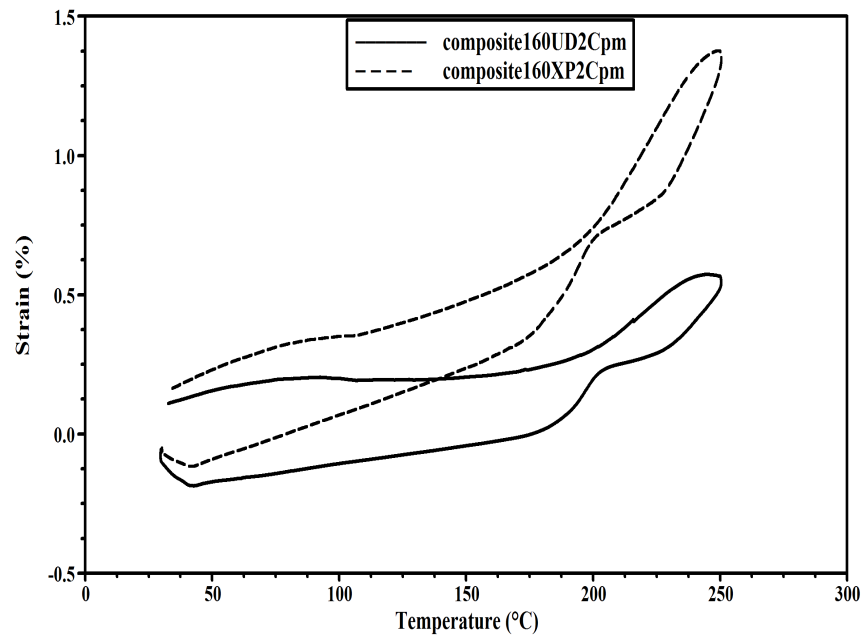


Figure 4.17. Strain vs. temperature graphs of cross-ply and unidirectional samples precured isothermally for 160°C; including both heating and cooling stages

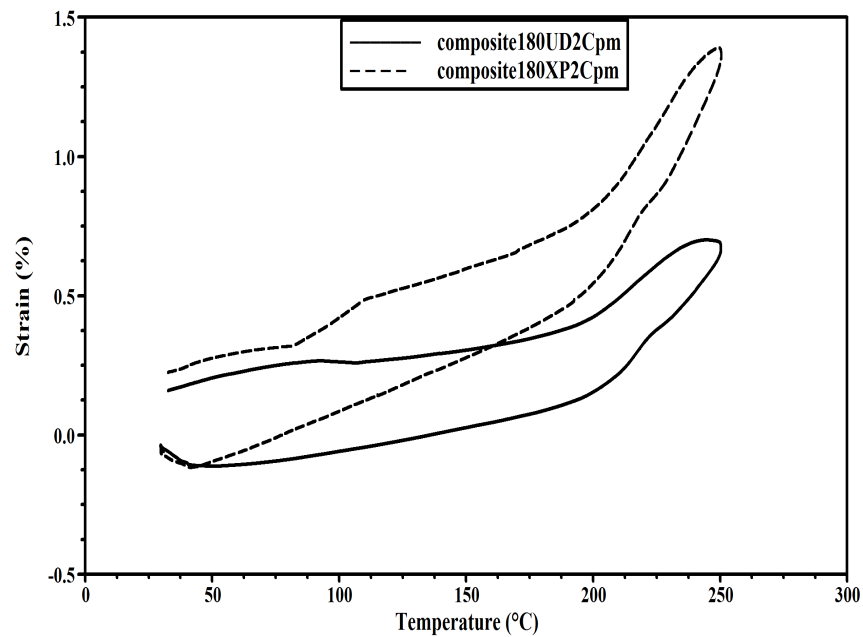


Figure 4.18. Strain vs. temperature graphs of cross-ply and unidirectional samples precured isothermally for 180°C; including both heating and cooling stages

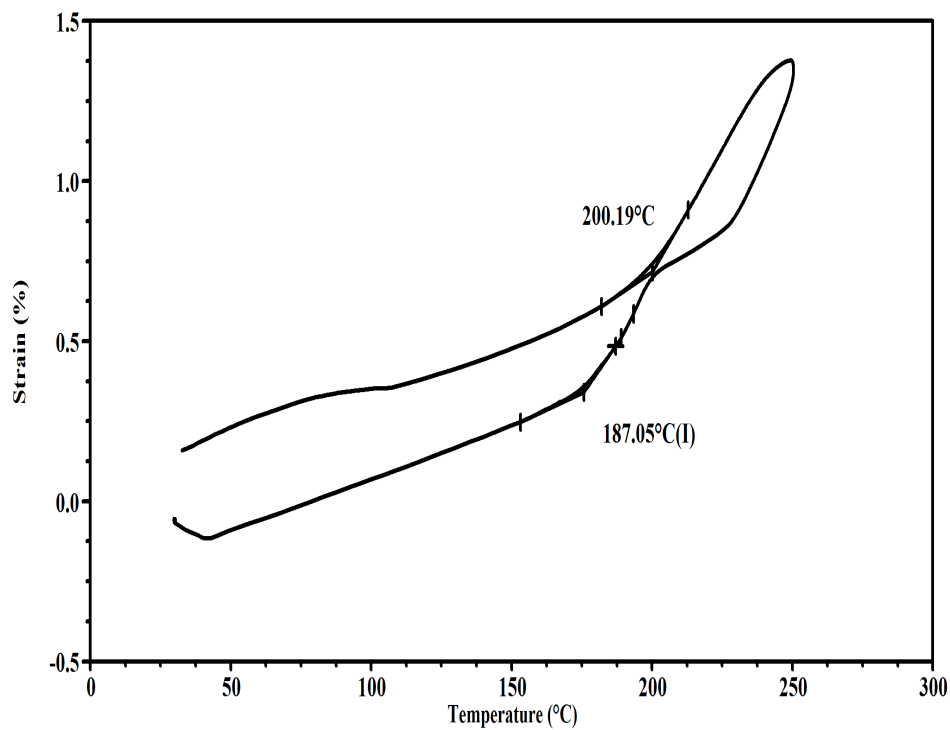


Figure 4.19. T_g calculations from the DMA experiments for 160XP sample as an example

Table 4.5. T_g values from DMA experiments

type of sample	Isothermal precure temperature (°C)	holding time at precure temperature (min)	T_g value while heating (°C)	T_g value while cooling (°C)
UD	120	360	132.8	203.4
UD	140	240	162.9	201.2
UD	160	180	185.4	201.2
UD	180	120	202.6	200.4
XP	120	360	140.0	200.1
XP	140	240	159.8	200.2
XP	160	180	180.3	200.2
XP	180	120	199.7	201.1

reaction (below T_g); the second is heating above T_g ; the third one is the cooling above the fully cured T_g ; the last one is the cooling below the fully cured T_g .

For all regions, a CTE value is calculated as in Figure 4.20. The calculated values are listed in Table 4.6 for each sample. Without some exceptions, the CTE values of XP samples are nearly twice of UD samples'. Also after the curing completed, the CTE values decreases.

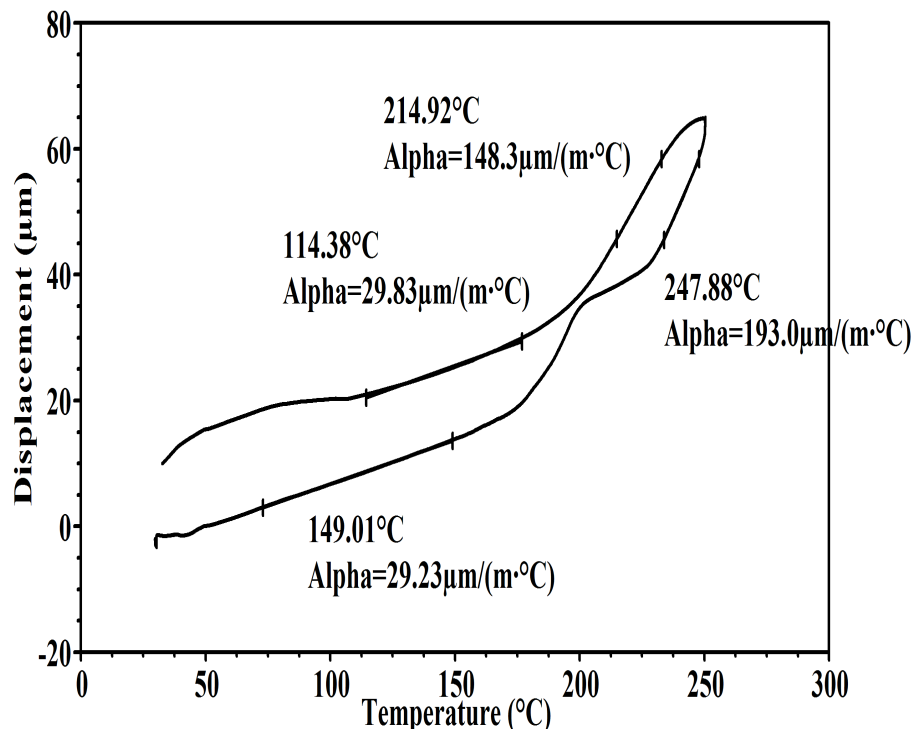


Figure 4.20. CTE calculations from the DMA experiments for 160XP sample as an example

4.2.2. Thermal expansion and cure shrinkage

The cure shrinkage process occurs at heating stage of the samples. Therefore, only the heating measurements of the experiments were analyzed. Figures 4.21, 4.22, 4.23, and 4.24 give the strain vs. time graphs of the samples during the heating stage in pairs of UD and XP.

The thermal strain responses of the unidirectional and crossply specimens cured at 160°C are given in Figure 4.14 together with the response of the empty clamp. It can

Table 4.6. CTE values from DMA experiments

type of sample	Isothermal precure temperature (°C)	CTE below T_g while heating ($\mu\text{m}/\text{m}\cdot^\circ\text{C}$)	CTE above T_g while heating ($\mu\text{m}/\text{m}\cdot^\circ\text{C}$)	CTE above T_g while cooling ($\mu\text{m}/\text{m}\cdot^\circ\text{C}$)	CTE below T_g while cooling ($\mu\text{m}/\text{m}\cdot^\circ\text{C}$)
UD	120	21.33	88.07	67.91	15.44
UD	140	19.39	108.1	76.54	19.26
UD	160	9.10	94.44	64.18	2.17
UD	180	13.26	97.90	68.14	9.85
XP	120	34.61	187.1	135.8	26.79
XP	140	38.89	200.7	147.8	32.76
XP	160	29.23	193.0	148.3	29.83
XP	180	34.86	184.4	135.2	24.99

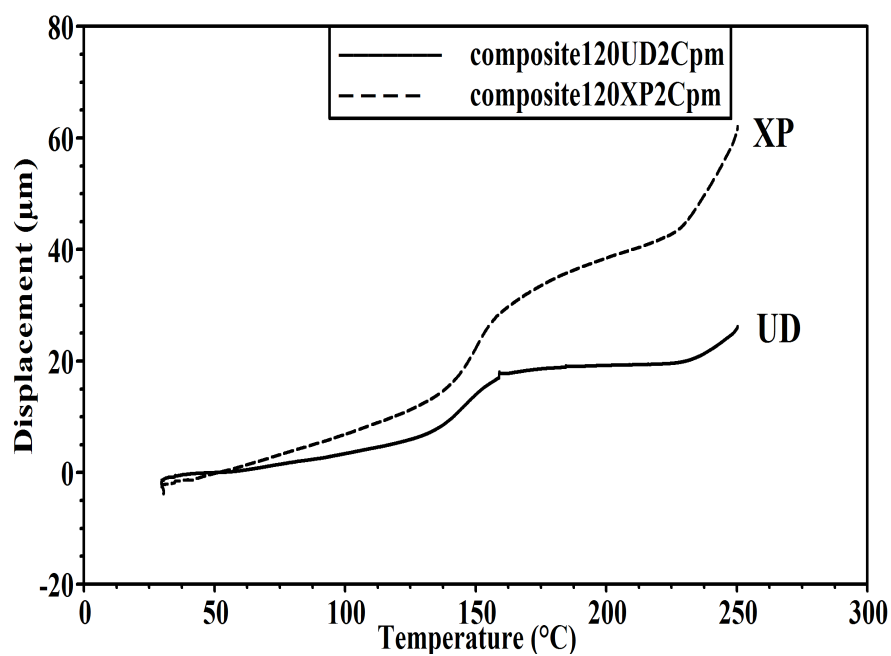


Figure 4.21. Strain vs. time graph of composites precured isothermally for 120°C

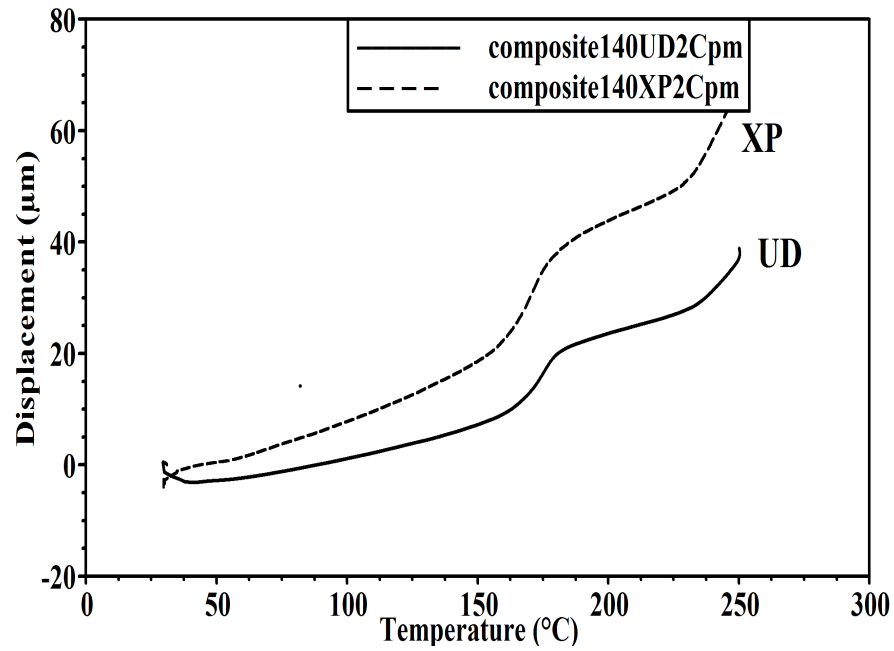


Figure 4.22. Strain vs. time graph of composites precured isothermally for 140°C

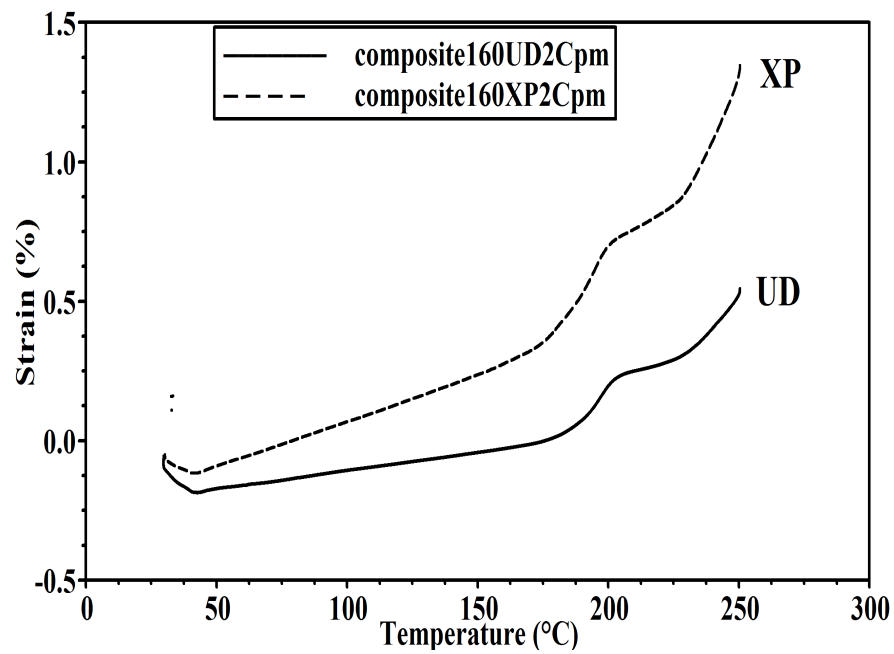


Figure 4.23. Strain vs. time graph of composites precured isothermally for 160°C

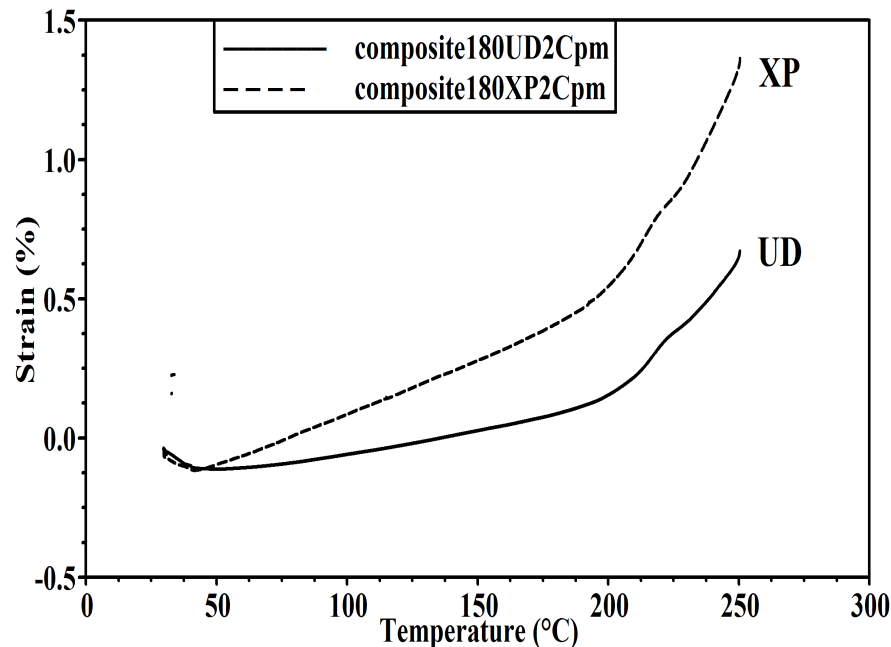


Figure 4.24. Strain vs. time graph of composites precured isothermally for 180°C

be seen that the clamp response is significant and the response of the samples should be corrected by using the clamp response as a baseline. As expected the response of the crossply sample is greater than the unidirectional sample due to the constraints imposed on the in-plane expansion due to the fibres running in both in-plane directions. The baseline corrected response of the crossply specimen cured at 160°C is shown in Figure 4.25. Here several features of the thermal strain response of the composite can be distinguished: During heating the partially cured composite expands due to increasing temperature and then undergoes a glassy-to-rubbery transformation; it then continues to expand in the rubbery phase with a greater CTE until the cure shrinkage starts to compete with the expansion. The reaction ends and since increasing temperature keeps the composite in the rubbery state, the composites continues expanding with almost the same rate as before the cure reaction. Cure shrinkage strain (ϵ_{cure}) can be found by extrapolating the expansion response before cure shrinkage and subtracting from this the thermal response after cure reaction as shown in Figure 4.25. Upon cooling, the composite undergoes a glass transition at around of fully cured composite.

The cure shrinkage strain values were found for each sample separately and listed

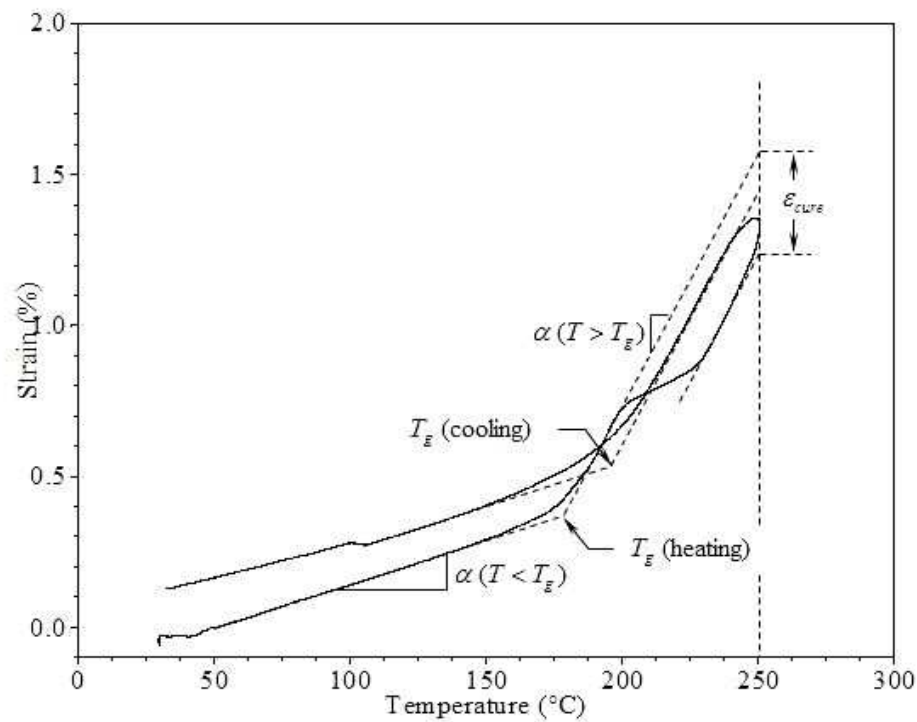


Figure 4.25. The method of calculating the cure shrinkage; displacement vs temperature graph of the sample precured at 140°C, as an example

in Table 4.7

4.2.3. Analysis of MRCC

For two composite samples, one UD and one XP laminate, the autoclave procedure was stopped after one hour isothermal hold at 120°C and the temperature of the composite were decreased to room temperature. The MRCC procedure starts with this stage and it proceeds by heating to 180°C at 2°C/min and isothermal holding for 2 hours. The precured samples were later heated according to the MRCC in the DMA equipment and the cure shrinkage values were calculated. To calculate the cure shrinkage, displacement versus time graphs of the empty clamp were subtracted from the response of the samples. After that, the difference between the maximum signal of the overall process and the stable signal of the isothermal holding were found as shown in Figure 4.26. Then this difference was divided to the thickness. The results were listed in Table 4.8. It can be seen from Figures 4.26 and 4.27 that the thermal expansion of the XP and UD samples are nearly the same. This behavior can be ex-

Table 4.7. Cure shrinkage values calculated from the thermal response of the samples during heating

Type of sample	Isothermal precure (temperature °C)	Holding time (min)	Through-the-thickness cure shrinkage strain
UD	120	360	0.7292%
UD	140	240	0.5617%
UD	160	180	0.2536%
UD	180	120	0.0538%
XP	120	360	1.069%
XP	140	240	0.9228%
XP	160	180	0.3843%
XP	180	120	0.0474%

plained by the fact that the resin is not gelled until the peak value and the cross-ply fibres do not exert any constraint in XP samples hence the individual layers expand in through-the-thickness direction and transverse direction giving the same expansion as in UD sample.

Table 4.8. Cure shrinkage strain values of MRCC

Type of sample	Cure shrinkage value
UD	0.5983%
XP	1.2107%

Figure 4.28 provides the strain values of two samples. The strain values were measured higher than the strain values of the precured samples, because of the uncured structure of the sample. One can see that the XP sample has higher cure shrinkage value, almost twice of the UD sample.

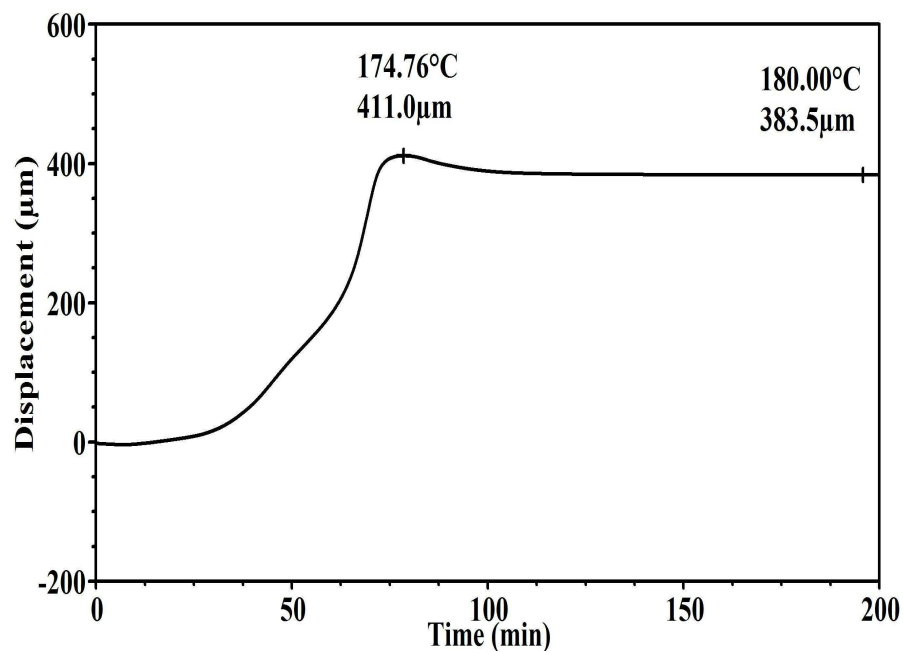


Figure 4.26. The method of calculating the cure shrinkage; displacement vs time graph of UD samples subjected to MRCC

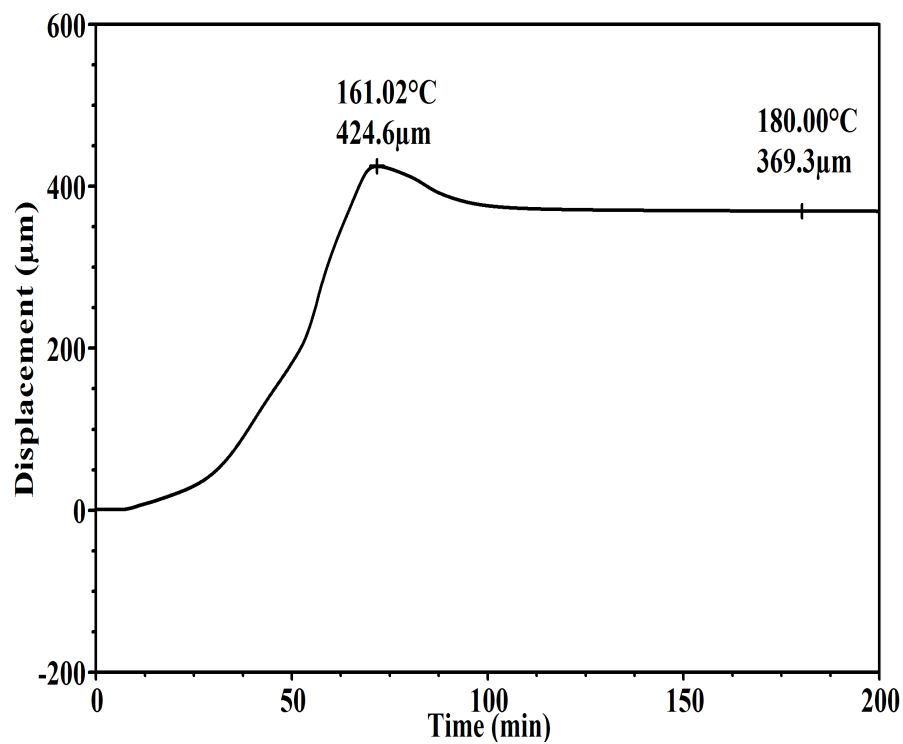


Figure 4.27. The method of calculating the cure shrinkage; displacement vs time graph of XP samples subjected to MRCC

4.2.4. Comparison of Results

As the final test, completely cured samples, one UD and one XP, were heated from room temperature up to 250°C at a heating rate of 2°C/min. Figure 4.29 shows the strain versus time graph of these samples. The strain values of the XP material is higher than the UD material. The T_g results were compared with DMA measurements in Table 4.9. The DMA results are the average of the T_g values measured from the cooling part of isothermal experiments. The Table 4.9 also includes the CTE values of the completely cured samples.

Table 4.9 shows that the T_g values of fully cured samples are almost same for heating and cooling. In Table 4.10 the T_g values from the DSC measurements are compared to the T_g values obtained by DMA during the heating stages of cycles. It can be seen that the two methods give almost the same values. All of these proves reliability of the measurements.

Table 4.9. Comparison of T_g values from the measurements of DMA experiments and the CTE values of the completely cured samples

Type of sample	Tg values obtained by		CTE below Tg ($\mu\text{m}/\text{m}\cdot^\circ\text{C}$)	CTE above Tg ($\mu\text{m}/\text{m}\cdot^\circ\text{C}$)
	Cooling of completely cured samples ($^\circ\text{C}$)	Heating of completely cured samples ($^\circ\text{C}$)		
UD	202.1	203.5	22.41	108.1
XP	200.3	198.4	46.83	154.8

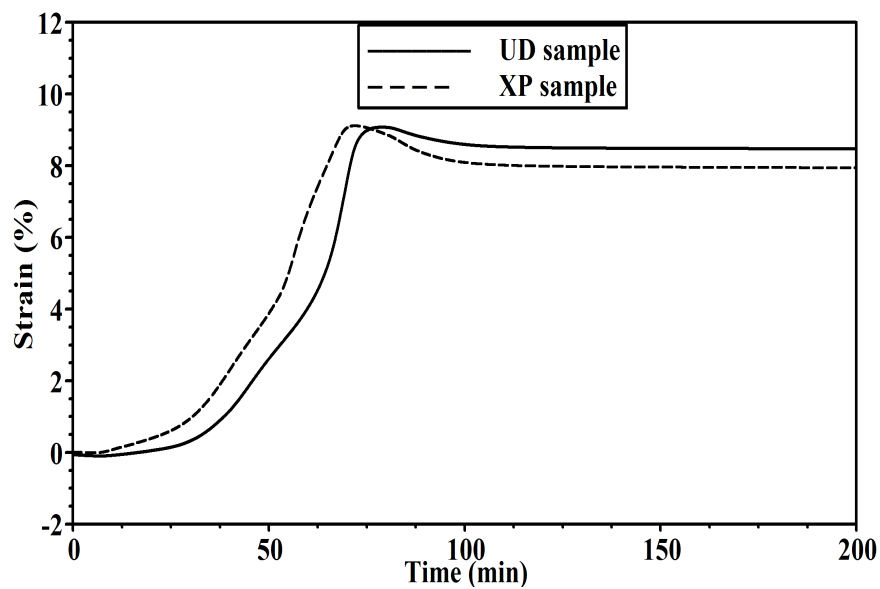


Figure 4.28. Strain vs. temperature graph of UD and XP samples subjected to MRCC

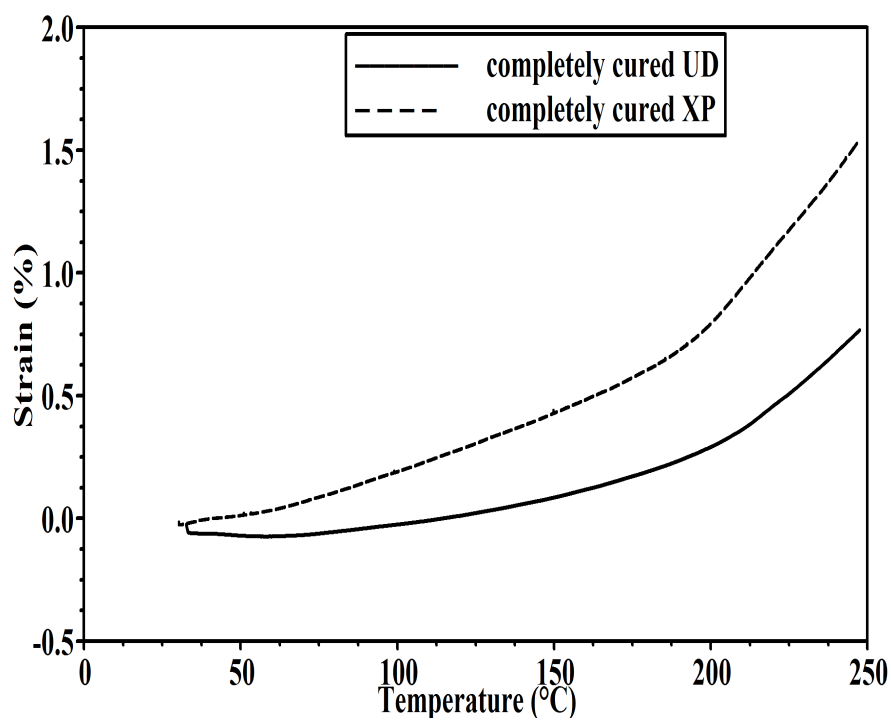


Figure 4.29. Strain vs. temperature graph of UD and XP samples of completely cured samples

Table 4.10. Comparison of T_g values from DSC and DMA experiments

Isothermal temperature (°C)	Glass Transition Temperature (T_g) (°C)	
	from DSC	from DMA (UD)
120	139.8	142.3
140	165.8	169.8
160	190.3	189.5
180	211.2	207.6

5. CONCLUSIONS

To understand and predict the properties of a composite upon curing, the cure kinetic model and the physical properties are required. In this work, the cure kinetics and cure shrinkage upon curing of an AS4/8552 epoxy resin system were studied. The study of the cure process is essential to optimize the cure cycle of epoxy prepreg in its applications. In this study, the dynamic and isothermal DSC method was applied to investigate the cure kinetics for the epoxy system of AS4/8552 and the degree of cure was calculated based on the heat of reaction.

Heat of curing heat of reaction can be found by integrating the heat flow curve. The dynamic curing heat of reaction are nearly same, but the isothermal cure heat of reaction increases with increasing cure temperature. According to the dynamic scans, the average heat of cure reaction was found to be 186.36 ± 18.74 J/g for the composite with 33 wt % resin. This corresponds to 559.08 J/g for the pure resin which is close to the values cited in the literature [32, 33]. The dynamic DSC experiments provide necessary information about the curing process. In the modeling part of the study, the selection of the most appropriate kinetic model and reliable estimation of its parameters is aimed. The simple n^{th} order kinetic equation could not fit the experimental data for every situation effectively. Instead, an autocatalytic-type kinetic equation was chosen to fit the experimental data.

The most appropriate kinetic model that produces a nearly perfect fit of the scans of all data sets corresponds to a process with a single-step parallel reaction with diffusion control. The whole curing process was treated to be composed of two cure reactions. The relationship between cure rate and degree of cure was simulated by the autocatalytic twelve-parameters model. The model is a modified version of the Sourour-Kamal equation [31]. The diffusion effect is incorporated into the model by Rabinowitch equation [13]. The chemical rate constant, which depend on the temperature, is described in the form of the Arrhenius equation. The diffusion rate constant is found by a modified WLF (Williams Landel Ferry) equation [14]. Multivariate kinetic

analysis were used to evaluate the parameters. The values of the fitted parameters are: $\log A_1 = 10.6047 \text{ s}^{-1}$, $E_1 = 129.8464 \text{ kJ/mol}$, $n_1 = 0.3946$, exponent $a_1 = 6.5163E^{-5}$, $\log K_{diff1} = -4.0229 \text{ s}^{-1}$, $\log A_2 = 5.0451 \text{ s}^{-1}$, $E_2 = 66.7952 \text{ kJ/mol}$, $n_2 = 1.2783$, Exponent $a_2 = 0.4535$, $\log K_{diff2} = -5.0136 \text{ s}^{-1}$, $C_1 = 8.2558$, and $C_2 = 27.1837$. The calculated heat flow values by this model agree very well with the DSC heat flow data in the entire cure process. The calculated total degree of cure gave good prediction of the experimental value. The model successfully predicted the appearance of a peak and a shoulder in the dynamic curing process.

The T_g values from the measurements of the isothermal experiments were found by reversible and nonreversible heat flow curves separately and are almost same. The residual heats of the samples of the isothermal study were measured to calculate the degree of cure. The isothermal experiments proved that the degree of cure increases with increasing cure temperature. The degree of cure values of isothermal experiments can be correctly predicted using the cure kinetics model.

In the second part of the study, the through-the-thickness strain response of the partially cured UD and XP epoxy laminates were measured by DMA. The strain values of XP samples were always higher than the UD's. The results of the measurements showed that the T_g values were proportional to the isothermal precure temperature and did not change in accordance with the type of sample (UD, XP). After the whole cure is completed, the T_g values were nearly same for all samples.

The thermosetting polymers with different degrees of cure will have different CTEs. The epoxy system experiences four distinct CTE values with respect to the T_g value during the cure reaction. The CTE above T_g is much larger than that below T_g . Without some exceptions, the CTE values of XP samples are nearly twice of UD samples'. Also after the curing is completed, the CTE values decreases.

During the whole cure cycle, the epoxy resin experiences chemical shrinkage as it crosslinks and physical shrinkage as it is cooled to room temperature. Chemical shrinkage due to the crosslinking reaction was found to be an important factor in

dimensional changes for epoxy resin systems. The cure shrinkage process occurs at the heating stage of the samples. The through-the-thickness cure shrinkage values were calculated from the displacement data of the samples. The results showed that as the isothermal precure temperature increased the cure shrinkage strain values decreased. Also, the cure shrinkage strain values of XP samples were higher than the UD samples'.

Two composite samples (one UD, one XP), which were heated to 120°C and held for one hour, were used to investigate the through-the-thickness cure shrinkage strain values during the MRCC. The thermal expansion of the XP and UD samples are nearly the same value of 9%. This behavior can be explained by the fact that the resin is not gelled until the peak value and the cross-ply fibres do not exert any constraint in XP samples hence the individual layers expand in through-the-thickness direction and transverse direction giving the same expansion as in UD sample [2]. The strain values were measured high as compared to the precured samples, because of the uncured structure of the sample. The through-the-thickness cure shrinkage strain values of UD and XP samples are 0.5983% and 1.211%, respectively. One can see that the XP sample has the higher cure shrinkage value, almost twice of UD sample.

The T_g values obtained by DMA and isothermal DSC experiments were compared and the values were found to be close to each other. Lastly, two fully cured samples (one UD, one XP) were heated up to 250°C and the T_g values confirmed the T_g values measured from the cooling part of the DMA experiments.

APPENDIX A: MORE DMA STUDY CURVES

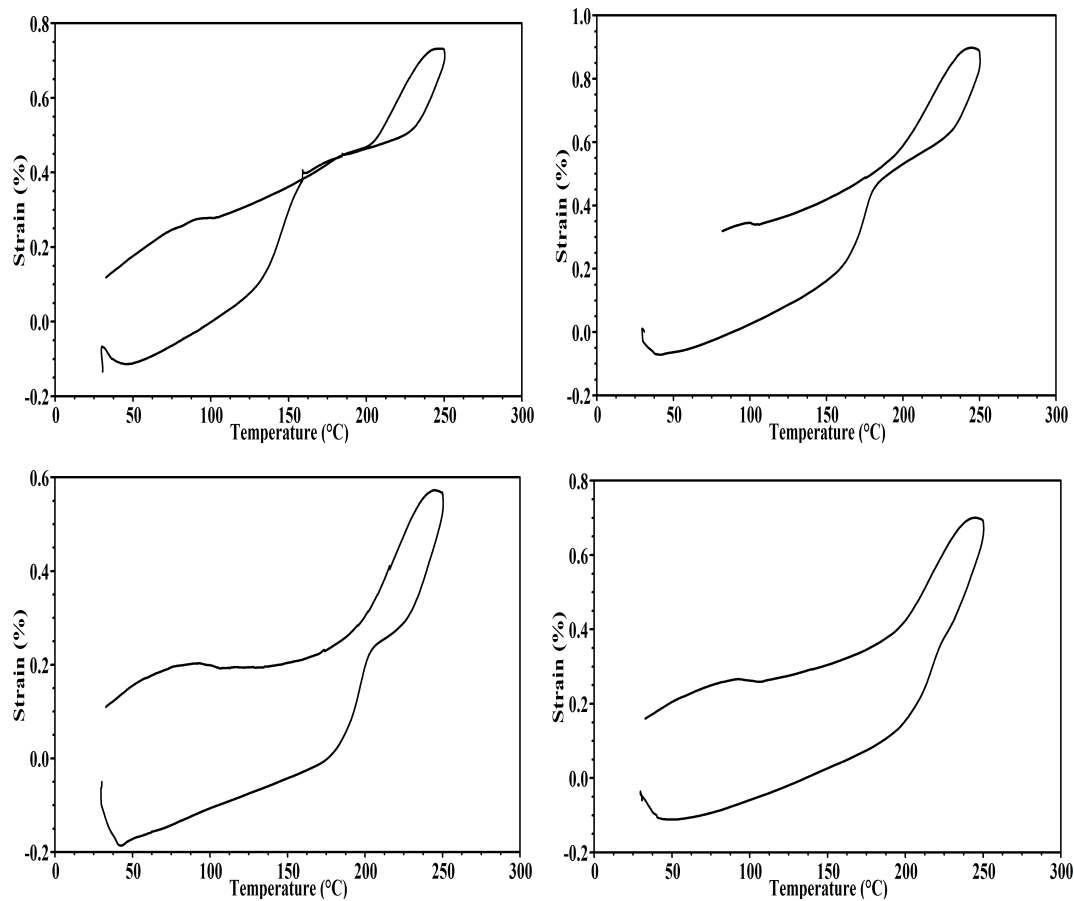


Figure A.1. Strain vs. temperature graphs of full cycles of unidirectional DMA samples precured isothermally for 120, 140, 160, and 180°C; including both heating and cooling stages

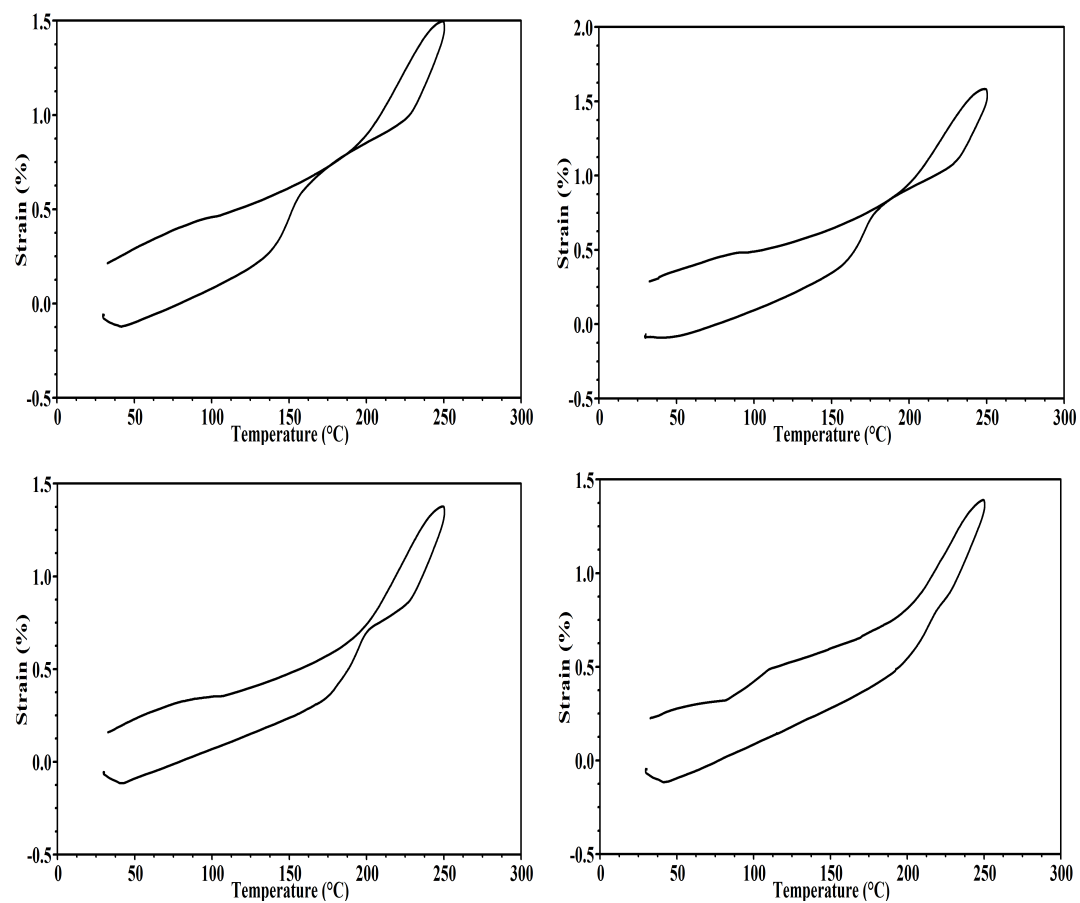


Figure A.2. Strain vs. temperature graphs of full cycles of unidirectional DMA samples precured isothermally for 120, 140, 160, and 180°C; including both heating and cooling stages

REFERENCES

1. Prime, R.B., Thermal Characterization of Polymer Materials, Academic Press, New York, 1982.
2. T.Garstka, N.Ersoy, K.D.Potter, M.R.Wisnom, In situ measurements of through-the-thickness strains during processing of AS4/8552 composite, Composites Part A: Applied Science and Manufacturing Volume 38, Issue 12, December 2007, pages 2517-2526
3. M.Opalicki, J.M.Kenny, L.Nicolas. Cure kinetics of neat and carbon-fiber-reinforced TGDDM/DDS Epoxy Systems. Journal of Applied Polymer Science, Vol.61, 1025-1037 (1996)
4. M.Buczek, D.Mason, C.W.Lee, A.Saunders. Proactive control of curing composites. Proceedings of the 44th International SAMPE symposium, Long Beach, CA, May 1999
5. J.Player, M.Roylance, W.Zukas, D.K.Roylance. UTL consolidation and out-of-autoclave curing of thick composite structures. 32nd International SAMPE Technical Conference, Boston, MA, USA; 5-9 Nov.2000, 757-767
6. P.Hubert, A.Johnston, A.Poursartip, K.Nelson. Cure kinetics and viscosity models for Hexcell 8552 epoxy resin. International SAMPE Symposium and Exhibition (2001), 46(2001:A Materials and Processing Odyssey, Book2), 2341-2354
7. V.Antonucci, M.Gioordano, S.I.Imparato, L.Nicolais. Autoclave manufacturing of thick composites. Polymer Composites, October 2002, Vol.23,No.5, 902-910
8. L.Sun, S.-S.Pang, A.M.Sterling, I.I.Negulescu, M.A.Stubblefield. Thermal analysis of curing process of epoxy prepreg. Journal of Applied Polymer Science, Vol.83, 1074-1083

9. L.Sun, S.-S.Pang, A.M.Sterling, I.I.Negulescu, M.A.Stubblefield. Dynamic modeling of curing process of epoxy prepreg. *Journal of Applied Polymer Science*, Vol.86, 1911-1923
10. N.Ersoy, K.Potter, M.R.Wisnom. Development of spring-in angle during cure of a thermosetting composite. *Composites Part A: Applied Science and Manufacturing* Volume 36, Issue 12, December 2005, 1700-1706
11. H.J. Flammersheim, J. Opfermann, Formal kinetic evaluation of reactions with partial diffusion control, *Thermochimica Acta* 337, 1999, 141-148
12. H.J. Flammersheim, J. Opfermann, Investigation of Epoxide Curing Reactions by Differential Scanning Calorimetry-Formal Kinetic Evaluation, *Macromol. Mater. Eng.* 2001, 286, 143-150
13. E.Rabinowitch, *Trans. Faraday Soc.* 1937, vol.33, 1225
14. C.W.Wise, W.D.Cook,A.A.Goodwin, *Polymer*, vol.38, 1997, 325
15. B. Yates, B.A. McCalla, L.N. Phillips, D.M. Kingston-Lee and K.F. Rogers, The thermal expansion of carbon fibre-reinforced plastics, *Journal of Material Science*, Vol.14,1979, pp. 1207-1217
16. I.M. Daniel, T.-M. Wang, D. Karalekas and J.T. Gotro, Determination of chemical cure shrinkage on composite laminates *J Composite Technol Res* 12 3 1990, pp. 172-176
17. T. Igarashi, S. Kondo, M. Kurokawa. Contractive stress of epoxy resin during isothermal curing. *Polymer* 1979; 20: 301-710.
18. J.D. Russell, Cure shrinkage of thermoset composites, *SAMPE Quart* 24 2 1993, pp. 28-33
19. Johnston AA. An integrated model of the development of process-induced defor-

- mation in autoclave processing of composite structures. PhD thesis. University of British Columbia, Department of Metals and Materials Engineering; 1997
20. M.A. Stone, B.K. Fink, T.A. Bogetti and J.W. Gillespie Jr., Thermo-chemical response of vinyl-ester resin, *Polym Eng Sci* 40 12 2000, pp. 2489-2497
 21. P. Prasatya, G.B. Mckenna and S.L. Simon, A viscoelastic model for predicting isotropic residual stresses in thermosetting materials: effect of processing parameters, *J Compos Mater* 35 10 2001, pp. 826-848
 22. Horng-Jer Tai, Chemical shrinkage and diffusion-controlled reaction in a cresol novolac epoxy, *Journal of Polymer Research*, Volume 7, Number 4, December 2000, 221-227
 23. B. Bilyeu, W. Brostow and K.P. Menard, Determination of volume changes during cure via void elimination and shrinkage of an epoxy prepreg using a quartz dilatometry cell, *Polimery* 46 2001, p. 799
 24. M. Zarrelli, I.K. Partridge and A. D'Amore, Warpage induced in bi-material specimens: coefficient of thermal expansion, chemical shrinkage and viscoelastic modulus evolution during cure, *Composites: Part A* Vol.37, 4, 2006, pp. 565-570
 25. C. Li, K. Potter and M.R. Wisnom, In situ measurement of chemical shrinkage of MY750 epoxy resin by a novel gravitometric method, *Composite Science and Technology* Vol.64, 2004, pp. 55-64
 26. A.C. Loos and G.S. Springer, Curing of epoxy matrix composites, *Journal of Composite Materials*, Vol. 17, No. 2, 135-169, 1983
 27. T.G. Gutowski, Z. Cai, S. Bauer, D. Boucher, J. Kingery and S.J. Wineman, Consolidation experiments for laminate composites, *Journal of Composite Materials*, Vol. 21, No. 7, 650-669 (1987)
 28. A. Poursartip and P. Hubert, A method for direct measurement of the fiber bed

compaction curve of composite prepregs, *Compos A* 32 2001, pp. 179-187

29. Pagliuso S, Warpaga A. Nightmare for composite parts producers. In: Hayashi T, Kawata K, Umekawa S, editors. *Progress in science and engineering of composites, ICCM 4*, 1982. p. 1617-23.
30. A.Kolbeck, T.Hauck, J.Jendryny, O.Hahn, S.Lang, No-Flow Underfill Process For Flip-Chip Assembly, 14th European Microelectronics and Packaging Conference and Exhibition, Germany, 23-25 June 2003
31. S.Sourour, M.R.Kamal, Differential Scanning Calorimetry of Epoxy Cure Kinetics, *Thermochem. Acta*, vol.14, 1976, pages 41-59
32. N. Ersoy, T. Garstka, K. Potter, M.R. Wisnom, M. Clegg, Micromechanical Models To Predict And Tests To Measure The Development Of As4/8552 Composite Properties Through Cure, to be published.
33. N. Ersoy, D. Porter, G. Stringer, Modelling The Development Of Structure And Physical Properties In 8552 Resin Through Cure, to be published.